HEAT & MASS TRANSFER ANALYSIS OF GOLD, TIN & INDIUM THIN LAYER DEPOSITION ON SURFACE

A Major Project Thesis submitted in partial fulfillment of the requirements for the award of the degree of

MASTER OF TECHNOLOGY

IN

THERMAL ENGINEERING

By

SHAILENDRA KUMAR GAUR

ROLL NO 2K12/THE/29

Under the guidance of

Dr. R.S.MISHRA

Department of Mechanical Engineering

Delhi Technological University, Delhi -110042

Session 2012-15

DEPARTMENT OF MECHANICAL ENGINEERING

Delhi Technological University, Delhi-110042

CERTIFICATE

This is to certify that the Major Project Thesis entitled "Heat and Mass Transfer Analysis of Gold, Tin & Indium Thin Layer Deposition on Surface" which is being submitted by Shri SHAILENDRA KUMAR GAUR, is the authentic record of student's own work carried by him out under my guidance and supervision for partial fulfillment of the award of the degree of Master of Technology in Thermal Engineering, Department of Mechanical Engineering, Delhi Technological University, Delhi.

(Dr. R.S.Mishra)

Professor,

Department of Mechanical Engg.

Delhi Technological University, Delhi

ACKNOWLEDGEMENT

It is a great pleasure to have the opportunity to extend my heartiest felt gratitude to everybody who helped me throughout the course of this minor project. It is distinct pleasure to express my deep sense of gratitude and indebtedness to my learned supervisor Dr. R.S.Mishra, Professor in the Department of Mechanical Engineering, Delhi Technological University, for his invaluable guidance, encouragement and patient review. His continuous inspiration only has enabled me to complete this thesis. I would also like to take this opportunity to present my sincere regards to my teachers for their kind support and encouragement. I am thankful to Director, SSPL and my colleagues from SSPL who give me support and help in doing this project work.

I am also thankful to my family members, friends and classmates for their unconditional support and motivation.

(SHAILENDRA KUMAR GAUR)

ROLL NO. 2K12/THE/29

6th Sem., M.Tech(Thermal)

Part-time

ABSTRACT

The surface temperature is required to specifying the temperature of the evaporating Gold, Tin and Indium source using constant elements for turn off the refinement in the post-processing settings. The present work represents the modeling of nanoscale Gold, Tin & Indium films by computing the film thickness, mass deposited on the substrate and mass transfer rate on silicon substrates with time dependent model using BDF solver. Gold is deposited by thermal evaporation process 34-38 nm by evaporating at temperature of 2000 °K in the vacuum of 50 Pa. Mass of gold deposited for 60 sec is 5.8×10^{-6} kg with mass transfer rate of 9.9×10^{-8} kg/sec. The SEM micrographs shows the smooth and uniformly distributed nanoscale gold film on silicon and the average grain size of gold is 12-30 nm. The XRD analysis shows the polycrystalline face centered cubic (fcc) structure in preferential (111) plane. Tin and Indium is evaporated from a resistively heated evaporator source at a temperature of 1855 °K and 1485 °K respectively in a pressure (vacuum) of 100 Pa onto silicon surface held on a fixed surface. The film thickness varies between 144 nm to 165 nm for Tin and 160 nm to 183 nm for Indium across the sample after 60 sec of deposition, with radial symmetry about the midpoint of the source. The film thickness as well as mass deposited at a point increases linearly with time. Like gold mass deposited & mass transfer rate for tin and indium also computed from the flux arriving on the substrate. Since the angular distribution is of particular interest in this model, by increasing the integration resolution to a maximum value for ensuring the most accurate angular resolution when computing the flux. The SEM micrographs of Tin and Indium at different magnifications shows the 100nm to 1microns grain size along the grain boundaries. Similarly, XRD analysis with Kα (wavelength 1.541874) shows the peaks of intensity at different 2θ angles for different orientations of planes with polycrystalline structure. The XRD of tin shows tetragonal polycrystalline structure in preferential (101) plane while XRD for indium shows tetragonal bcc structure in preferential (103) plane for tin & indium thickness of 164 nm, 183 nm respectively. Deposited gold, tin & indium film thickness measured from Dektek surface profiler at different points on the substrate surface.

Keywords: Physical Vapor Deposition, Modeling, Film Thickness Simulation, Tin Evaporation, Indium Evporation, Thin Film Deposition

CONTENTS

NOMENCLATURE

Tc	room temperature in chamber (°K)
Te	temperature of evaporation (°K)
P	pressure (Pa)
r	distance between source and target (mm)
D	diameter of vapor atom (Å)
k_B	Boltzman constant
t	nominal film thickness
Rm	mass deposition rate per unit area of source surface
M	evaporant gram molecular mass (gm)
Pe	evaporant Vapor pressure(Pa)
W	width of substrate
θ	angle between source and a point at substrate
A	cross-sectional area
α_v	evaporation coefficient (dimensionless)
J	outgoing(emitted) flux (molecules/m ^{2}/s
S	sticking coefficient
G	incident molecular flux in molecules/m^2/s
N_A	Avagadro's number
n_{ads}	number of adsorbed moles in mol/m^2
D	desorption rate in mol/ m^2/s
M_n	mean molar mass

LIST OF FIGURES

LIST OF TABLES

1.1Definition

Physical methods produce the atoms that deposit on the substrate by evaporation and sputtering. Sometimes called **vacuum deposition** because the process is usually done in an evacuated chamber PVD is used for metals while dielectrics can be deposited using specialized equipments. It rely on thermal energy supplied to the crucible or boat to evaporate atoms. Evaporated atoms travel through the evacuated space between the source and the sample and stick to the sample. Few, if any, chemical reactions occur due to low pressure can force a reaction by flowing a gas near the crucible. Surface reactions usually occur very rapidly and there is very little rearrangement of the surface atoms after sticking. Thickness uniformity and shadowing by surface topography, and step coverage are issues. Ali Moarrefzadeh et al. [1] discussed that Physical vapor deposition (PVD) includes a wide range of vacuum coating processes in which material is physically taken out from a source by evaporation or sputtering, transported through a vacuum or partial vacuum by the energy of the vapor particles, and condensed as a film on the surfaces of appropriately placed parts or substrates. A group of very versatile coating processes in which a material is converted to its vapor phases in a vacuum chamber and condensed onto a substrate surface as a very thin film(upto 1 μm thickness). The deposition of thin film layers from the vapor phase is done through several methods. We study and analyze the physical vapor deposition (PVD) techniques and equipments that are in common use in the large scale production of coatings that find uses in the optical, display, decorative, tribological, and energy-generating /saving industries. Evaporating materials are classified as dielectric compounds, metals, alloys, or mixtures. The same evaporant material can exhibit different optical, electrical, and mechanical properties depending on the deposition process. Titanium oxide is a unique example of a metal oxide compound that, depending on deposition process parameters, can be made into film layers that are: transparent, electrically conductive, chemically reactive to light and bio- agents, chemically inert, or exhibit spectrally selectively absorption. The dependent parameters are starting composition, oxidation state, and crystalline structure and packing density. PVD techniques used generally are basically two in nature: thermal evaporation by resistively heating or by using an electron- beam heating, and sputtering, a no thermal process. P.S.Raghupathi et.al.[28] and Haichuan Mu et.al. [29] discussed that the thermal evaporation deposition rate influence the structural, electrical & optical properties of thin film deposited like in case of Indium-tin-oxide(ITO).Alterations and accompaniments are made to the basic PVD techniques to permit different coating materials and substrate types to be included

additions designed to alter the growth nano-structure or composition of the film through control of the dependent variables listed above include bombardment of the growing film by high energy inert- or and reactive ions, substrate heating, atmosphere composition and partial pressure, rate, and vapor incidence angle. A further important variable contribution to the nucleation and self-assembling growth structure of the condensing atoms, that we have discussed frequently, is the condition both chemical and physical of the substrate surface (PVD process shown in following figure 1.1

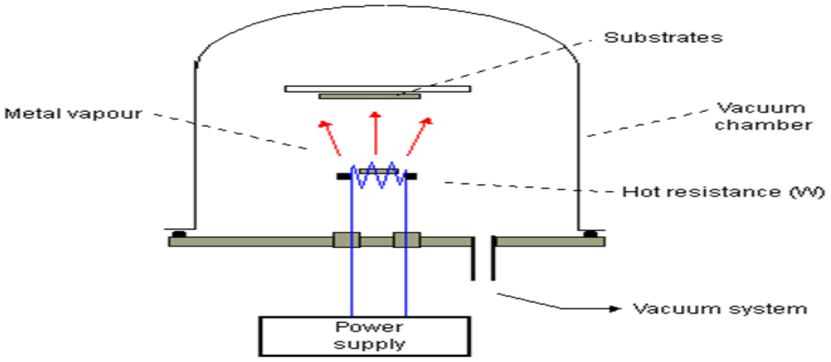

Figure 1.1 Vacuum coating process diagram

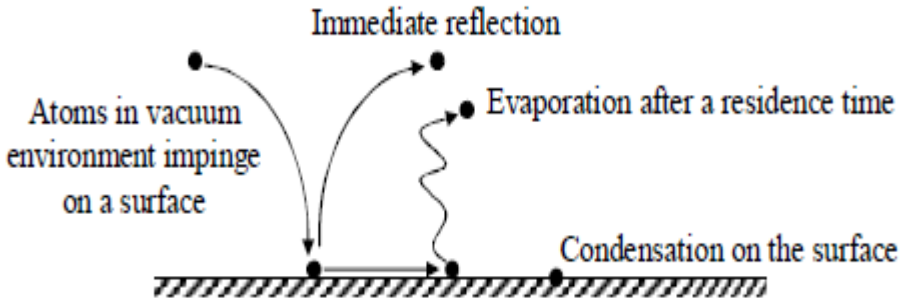

Figure 1.2 Mechanism of Thermal evaporation process (ref.[1])

PVD Film Evaluation

Deposited films are typically evaluated for visual defects, thickness, and adhesion. Visual defects such as bare spots, small voids, incorporated flakes, or debris can be observed with a stereo microscope having a magnification of 10 to 100 times. Film thickness is generally measured by one of the following methods: Thickness of film as modeled can be simulated experimentally with dektek surface profilometer with diamond size of 12.5µm radius stylus. Polished metallurgical micro sections are used to microscopically observe the coating thickness on various part surfaces. This method is the most direct way to determine thickness uniformity. Beta (high-energy electron) backscatter instruments are used to measure the film thickness nondestructively. This is an indirect method that requires calibration with a known standard; substantial errors can be made in

measuring the film thickness on curved surfaces if care is not exercised. A ball-crater instrument can be used to polish through the surface of a coating. The relationship between the diameter of the polishing ball, the maximum diameter that shows the effects of polishing, and the diameter of the substrate area that is exposed by polishing is used to calculate the thickness. Coatings that are up to 120 m-in. (3Mm) thick can be measured with an accuracy of±4 m-in. (±0.1 Mm) without difficulty on relatively smooth, flat or cylindrical surfaces. The adhesion between coating and substrate is difficult to measure directly for highly adherent films; pull tape tests capable of measuring yield strengths that are typical of metals and PVD hard coatings on metals have not been developed.

1.2 Thermal Evaporation Process

In thermal evaporation process, load the source material-to-be-deposited (evaporant) into the container (crucible). Then resistively heat the container (tungsten or molybdenum boat) containing source to high temperature i.e. evaporation temperature depending upon the material to be deposited. The source material evaporates and evaporant vapor transports to and impinges on the surface of the substrate. Evaporant condenses on and is adsorbed by the surface.

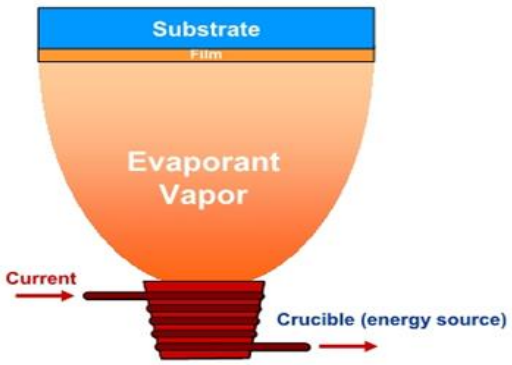

Figure 1.3 Thermal evaporation processes (ref. CIMS applied physics)

Furthur study shows that evaporation used in thin film deposition can be done by:

a) Thermal evaporation
b) E-beam evaporation

Thermal evaporation is very old, easy, reliable and good method of deposition while E-beam evaporation requires elaborate and complex system. Moreover high velocity electron creates surface defects and stress on the deposited surface**.** The choice of any particular heater design is dependent on a number of factors related to the material to be evaporated i.e. the form in which it is available: granules, powder, wire or sheet, and its evaporation behavior whether it wets or forms alloys with the heater material or volatilizers form a molten globule. In, general the evaporation takes place according to Knudens's cosine law. This is the gas-kinetic analogy to Lambert's law for

radiation. To obtain a specified film distribution one has to consider the shape of the receiving surface and the arrangement of the vapor source or sources of evaporation from the source, viz. whether evaporation takes place uniformly in all directions or if there are any preferred directions.

Assumptions:

1. The evaporation is carried out at a sufficiently low gas pressure for the scattering of vapor molecules by collisions with gas molecules to be negligible.
2. The vapor intensity is so low that the effect of collisions between vapor molecules in the vicinity of the source can be neglected.
3. The assumption is made that all fluxes in the model change much more slowly than the transit time of the molecules across the geometry. At every time step the solver assumes that flux emitted from a source boundary arrives instantaneously at a destination boundary.
4. The every vapor molecule striking the receiving surface condenses on first impact.

The above assumptions are necessary conditions for Knudsen's cosine law to be applicable.

1.2 Objectives of the Present Research Work

The present work has been performed to achieve the following objectives:

1. To find out the deposited film thickness on the silicon substrate and variation of the thickness across the surface of sample.
2. To find out the mass deposited on the silicon substrate and its variation with time
3. To find out the mass deposition rate on the silicon substrate with time
4. Micrograph and microstructure analysis of the deposited film by SEM and XRD for grain size & uniformity along grain boundaries and orientation of crystal planes.
5. Measurement of deposited film thickness at different points on the substrate surface from Dektek surface profiler and comparison with the thickness value given by DTM(a piezoelectric transducer)

Chapter 2

LITERATURE REVIEW

The nanoscale gold film thickness has found newer capabilities in different fields of science & technology such as coating glasses/mica to change their properties and many coloured optical coding for biological assays. Gold nanometer thick film is being used to enhance electroluminescence and quantum efficiency in light emitting diodes. Besides signal amplification, nanometer thick gold film evoluted new types of new sensors that are capable of detecting very small amounts of analytes such as chemical vapors in the scale of few ppm. Adeleh Granmayeh Rad et al [2] discussed the usage of gold nano film is in making advanced dyes and pigments. Sometimes gold nano film has been used to dye textiles, support to supply clean energy (by solar cell) and high density data storage (flash memories and discs). Gold nanoscale film quality of non-toxic and biocompatibility both in vivo and in vitro environments makes useful in bio-medical applications. The unique properties of gold nanoscale structured materials supply good opportunity for coordinating biological identification events with electronic signal transduction and for making an evolution of bioelectronics devices with newer features. Gold in nanoscales have been found for potential candidates to support in photo-thermal therapy and radiotherapy. Optical and electronic properties of gold can be utilized to improve the contrast in molecular imaging for the detection of cancer initially. Gold-based technologies also help to facilitate a ultimate needle-free delivery system, a technique that used gold and permitted vaccines to be supplied through the skin producing use of the fact that small particles can go through gaps between cells while large ones cannot. Gold nanoscale- based technologies give solution to some of environmentally great issues, such as ecofriendly production methods, pollution control and water purification. No doubt gold is really one of the non- reactive metals, and it is resistant to oxidation**.** Ragini Raj Singh et al. [3] discussed gold is also used in Photovoltaic HgCdTe Mid wavelength Infra-red detector to make ohmic contacts to find out the passivation characterstics of CdS/HgCdTe structure using C-V measurements. Wenjun Zhou et.al [4] discussed the Chemical vapour deposition (CVD) generally uses a gas-phase precursor, often a halide or hydride of the element to be deposited. In the case of MOCVD, an organometallic gas is used. Commercial techniques often use very low pressures of precursor gas. The chamber is first evacuated to a vacuum of around 5m torr and substrate temperature fixed to 350°C. Now evaporator is resistively heated to a temperature of about 160°Cto start volatilization of the precursor. The deposited precursor then thermally decomposes into pure gold by a reaction above 300°C. The thickness of the gold film can be controlled by adjusting the

amount of precursor, the temperature of the deposition chamber, and the location of the samples to be coated relative to the inlet of the evaporator into the deposition chamber. Generally gold precursor is thermally stable between 150 and 300 °C. Keewah Chan et al [5] discussed that gold can be deposited on silicon or quartz by rf sputtering by using DC sputter coating system. The rf power can of several hundred watt, substrate temperature about 300 °C with a vacuum of 1mbar order or better for time depending upon the thickness required, say for nanometer thickness 1 hour. Carl E. Larson et al. [6] discussed that gold deposition of high purity gold onto various substrates from dimethyl-2fl- pentandionato gold (III), Me2Au (acac), by localized, laser- induced (photothermal) chemical vapor deposition. CVD of gold from dimethyl-(1,1,1-trifluoro-2,4-pentandionato) gold (III) and dimethyl-(1,1,1,5,5,5-hexafluoro-2,4- pentandionato) gold(III),Me2Au(tfac) and Me2Au(hfac) complex can be done in a stainless steel vacuum chamber evacuated by a turbomolecular/diffusion/cryo pump to a base pressure of < 10 -6 torr. A flow of argon or nitrogen carrier gas through a Pyrex vessel containing the gold complex at room temperature is used to deliver the organogold precursor into the chamber through stainless steel lines. Chamber vacuum and carrier gas flow rate could be varied independently. Deposition proceeds on a substrate placed in the chamber in the flow path of the carrier gas and heated by a copper block heater with temperature controller. Miroslav Gojo et al [7] discussed that gold can be deposited in a thermostatically controlled electode cells in a electrodeposition Cell has two openings, one for thermometer another for nitrogen inlet for purging the oxygen out of the electrolyte keeping pH value 5 to 7 and each silicon wafer piece coated and alloyed with gold as working electrode, filled with chosen electrolyte warmed upto a given temperature and purged with nitrogen. Gold deposited by electrochemical method has higher purity, lower permeability and good adhesion to the substrate. Anne-Felicie Lamic-Humblot et al[8] discussed that gold can be very easily deposited at ambient pressure and in distilled water with magnetic rod stirring , followed by thermal treatment from tetrachloroauric acid and urea. T. Donnely et.al.[9] discussed that gold on nano scale can be deposited on Si and sapphire by pulse laser deposition(PLD) by Nd : laser operating at 1064, 20Hz and pulse length of 6 nano sec used in a vacuum. The PLD deposited gold nano scale film is characterized and below 5 nm equivalent thickness AFM confirms the nano particles while optical measurement shows surface plasmon resonance shifts to longer wavelengths with increasing thickness. X.Zhang et.al.[10] discussed that gold film deposited on a quartz crystal ablated by excimer laser and found that ablation rate is more than two order higher than surface vaporization model prediction. Also this ablation rate strictly dependent on gas pressure. Anna Schaub et.al [11] discussed that gold deposited by vacuum evaporation on glass substrate without heating glass and with heated glass. Further characterization is done of those deposited films i.e. without heated glass, without heated glass followed by annealing at 300 °C and heated glass, finding that heating during evaporation results in decrease in roughness and morphology changes

with heating and annealing conditions. Behrang Moazzez et.al.[12] stated that the good adhesion gold on electronic device such as sensors, MEMS etc. making surface can be improved by applying gold deposition step on SU-8 photo resist prior to UV exposure but after the pre-bake step of SU-8 processing. Maxime Gougis et. al. [13] discussed the gold deposition by pulse laser ablation on carbon nanotube electrode but with in presence of oxygen and confirmed the non oxide formation by characterization. C. Celed´on et.al.[14] discussed that the surface roughness affects on the energy straggling associated to the energy loss distributions of protons transmitted through a self supported metallic thin foil. Hartmann Hieber and Karin Pape [15] discussed the ageing of gold stating that degradation under thermal and electrical fault and in contaminated conditions is very low that is why gold is better than other metallization. Adam Proszynski et al [16] discussed that stress is developed during vacuum evaporation of gold nanometer film which can be reduced by post annealing process and further characterized the film for confirmation. Thin tin oxide deposited surface is very useful in industries due to their properties such as n-type Semi-conductor character, high optical transmission in visible range, high reflectivity; in the infra-red as well as good chemical resistance. Thus they can be used to form transparent and chemically stable thermal barriers. R.S. Mishra et. al.[36] stated that gold on nanoscale 34-38nm can deposited by thermal evaporation process at a vacuum of $1x\ 10^{-6}$ mbar with thickness maximum at the centre of silicon substrate following cosine distribution law. C. R. Zamarreñoa et al. [17] discussed the fabrication of optical fiber refractometers based on indium tin oxide (ITO) coatings with good sensitivity in the visible spectral region. ITO thin-films have been deposited by using sputtering mechanism and employing a rotating mechanism that makes possible the fabrication of smooth homogeneous coatings onto the optical fiber core. Souad Laghrib et al. [18] discussed the vacuum evaporation of Tin followed by annealing with oxygen flow to obtain Tin oxide thin layers. He did a lot of experiments by varying the deposited Tin thickness as well as annealing conditions by varying annealing temperature with different duration and found that at high temperature annealing forms nanocrystalline tin oxide. Sea-Way Jan et al. [19] discussed the formation of indium tin oxide by first metal tin and indium deposition in oxygen in vacuum coating system maintain vacuum of $1x\ 10^{-6}$ torr by combination of rotary and diffusion pump. Further studied the deposited film through XRD, SEM, TEM, Hall measurement and found polycrystalline film with bcc structure. This film is used in front panels in liquid crystal and electroluminescence displays, transparent heating elements, high-efficiency ITO/GaAs and ITO/InP solar cells, blue light electroluminescence etc. D.Bruce Buchholz et al. [20] discussed the few nm thin layer of indium oxide by pulse layer deposition method and studied formation of crystalline and amorphous with variation of temperature and density variation. Alexandu C.Fechete et al.[21] discussed the indium oxided nanostructures in the form of nanobelts and nanorods with few microns length and 200 nm width developed by thermal evaporation on silicon substrates with and without presence of gold catalysts

in temperature range of 600- 900˚ C in which growth process involved are vapor-solid and vapor-liquid-solid and the nanobelts are appx.10-200 nm wide and few micrometers long at 750˚C when no catalyst while when Au catalyst is used, homogenous scattered nanorods obtained at 900˚C. C.A.Pan et al. [22] discussed that high quality and high conductive indium oxide films prepared by thermal evaporation from In and In2O3 source in vacuum chamber with low pressure of O2 of which properties comparable to tin doped indium oxide films. Its low resistivity is as a result of excellent electron mobility (~70cm^2 /V sec) though the electron concentration is rather high which makes it a perfect for fabrication of semi-conductor device. Burstein shifts due to high electron density in conduction band also seen. B.Maniscalco et al. [23] discussed the thin film thickness measurement of Indium Tin Oxide made using coherence correlation interferometry. Optical transmission over the whole visible spectra with a steep decrease 380 nm. Indium Tin Oxide (ITO) is widely used in applications such as touch screens, LCD and OLED displays, thin film photovoltaics. M.Trzcinski et al [24] discussed the alloy formation of ultrathin Ag and In layers deposited on W(100) starting at room temperature and finished after a small annealing at 600 K. The alloying process is originally geometrical and no major difference between 2D layered alloys and 3D bulk alloys can be found. D. Kalhor et.al. [25] discussed that the post-deposition annealing at 300 °C of ITO film used in multi layer film ITO/Ag/ITO at glass substrate improves the opto-electronic properties of thermal evaporated films. Mika Yamaguchi et.al.[26] stated that Sn doped ITO is very useful in commercial use due to property of transparent to visible light and electrical conductivity. Artorn Pokaipisit et.al. [27] discussed that annealing at different temperature of ITO film e.g at 200, 250, 300 and 350 °C increases the transmittance and grain size with increasing the annealing temperature and lower resistivity which makes it suitable for use in electronic device fabrication. Shailendra Kumar Gaur et.al.[37] discussed that films of tin and indium nano scale tin & indium films by computing the film thickness, mass deposited on the substrate and mass transfer rate with time dependent model using BDF solver. Shailendra Kumar Gaur et. al.[38] stated that COMSOL modeling can also be used for induction heating of copper cylinder with water cooling based on turbulent flow and instantaneous water mixing. By modeling through this we can easily get temperature distribution inside copper cylinder and water cooling based on turbulent flow. Varieties of coatings can be deposited such as metals, alloys, ceramics and other inorganic compounds, and even certain polymers. Deposition can be done onto the varieties of substrates such as metals, glass, and plastics.

The properties of atavistically deposited films depend strongly on:

- The material being deposited
- Substrate surface chemistry and morphology
- The surface preparation process

The details of deposition process and the deposition parameters :

- mean free path of evaporant
- source to substrate distance
- vapour pressure of evaporatnt
- sticking coefficient

Condensation and nucleation- Atoms that impinge on a surface in a vacuum environment may be reflected immediately, re-evaporate after a residence time, or condense on the surface shown in figure 1.2 Mean free path is the minimum distance between two successive collisions and is given by formula depending upon the vacuum in the chamber :

$$\lambda = \frac{k_B T_c}{\sqrt{2}\pi \cdot P \cdot d^2}$$

where T – usually room temp. of chamber

P –Vacuum in chamber

D - diameter of vapor atom ~2-5 Å

At 300 K

$$\lambda = \frac{5x10^{-3}}{P_T(Torr)} cm$$

Based on this mean free path source to substrate distance is optimized for constant flux and better deposited film quality. Sticking coefficient is defined as the ratio of the condensing atoms to impinging atoms. If the atoms do not immediately react with the surface, they will have some degree of surface mobility over the surface before they condense. Re-evaporation is a function of bonding energy between the adatom and the surface, the surface temperature, and the flux of mobile adatoms. Example: The deposition of cadmium on a steel surface having a temperature greater than about 200 ˚C will result in total re-evaporation of the cadmium.

Surface mobility

The energy of the atom, atom-surface interaction (chemical bonding), and the temperature of the surface influence the capability of an atom on a surface. The mobility on a surface can change because of variations in chemistry or crystallography. The various crystallographic plates of a surface have different surface free energies that influence the surface diffusion. Atoms condense on a surface by losing energy. They lose energy by:

-forming and breaking chemical bonds with the substrate atoms.

-Finding preferential nucleation sites (lattice defects, atoms steps, and impurities)

-interacting with another diffusing surface atoms (same species)

-Colliding or reacting with adsorbed surface species.

Atoms form nuclei after condensation. Homogenous nucleation is said to occur if the surface is of same material as the deposition atoms and if they are different materials, the process is called heterogeneous. In semiconductor field, heterogeneous nucleation forms hetero- junctions. G.H. Gilmer [30] et al discussed that **t**hree types of nucleation mechanisms have been identified; they differ according to nature of interaction between the posited atoms and the substrate material:

Frank-Van der Merwe mechanism leading to a monolayer-by-monolayer growth (layer growth; ideal epitaxy).

Volmer-Weber (V-W) mechanism, characterized by a three-dimensional nucleation and growth (island growth).

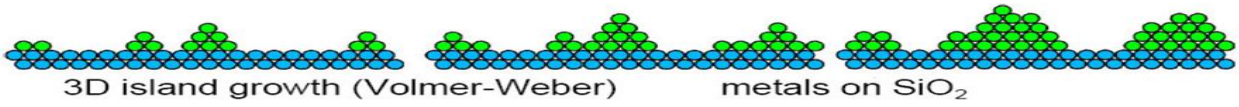

Stranski-Krastanov (S-K) mechanism, where an altered surface layer is formed by reaction with the deposited material to generate a strained or pseuomorphic structure, followed by nucleation on this layer (Layer + island growth)

Nuclei coalescence and agglomeration The nuclei develop by collecting atoms that diffuse over the surface. Isolated nuclei grow laterally and vertically on the surface to form a continuous film and to form a continuous film less amount of material is needed if nucleation density is high. The principal growth mode of nuclei may be: -laterally over the substrate surface (wetting growth) such as gold on copper and chromium, iron on W-O surfaces, and titanium on SiO2 the nuclei may prefer to grow in a vertical mode (dewetting growth) such as nickel and copper on W-O surfaces, and gold on carbon, Al2O3, and SiO2. Growth and coalescence of the nuclei can leave interfacial voids or structural discontinuities at the interface, particularly if there is no chemical interaction between the nuclei and substrate material and dewetting growth occurs.

2.2 Scope of Present Work

Though a lot of research work has been done on the evolution of gold, tin and indium film deposited on nanoscale or higher thickness by different deposition process through different heating sources (resistively, sputtering,E-beam,magnetron, radio frequency) in different baskets/crucibles at different temperatures and modeled mostly with direct simulation monte carlo. Also these methods solve in the volumes of the modeled and geometries. Number densities found to be not accurate and

precise. Ineligible simulation for the accurate modeling of low pressure, low velocity gas flows in complex geometries. These studies subjected to statistical scatter. Moreover, these could not completely explained free molecular flow interface and applied dsmc computes the trajectories of large numbers of randomized particles through the system, but introduces statistical noise to the modeling process and also the method is slower. Moreover, present work emphasis on the thermal and mass transfer of thermal evaporation process as well as structural analysis of deposited thin films leading to better optimization of thermal evaporation process and development of suitable electronic device fabrication applications.

Experimental Set-up for deposition of Gold, Tin & Indium:

The island films were prepared using a laboratory thermal evaporation setup as shown in figure 3.1 working at residual vacuum of (2.5 - 4) × 10^{-6} mbar. The deposition setup was equipped with the two-stage vacuum system based on the diffusion pump (oil based), turbomolecular or cryopump along with rotary vane pump or rotary screw pump (oil free). In case of oil based pumps the ultimate vacuum achieved in the system depends upon the vapor pressure of the oil used in pumps, generally Silicone based oils are used to achieve vacuum of 1.0 x 10^{-6} or higher order in the chamber.

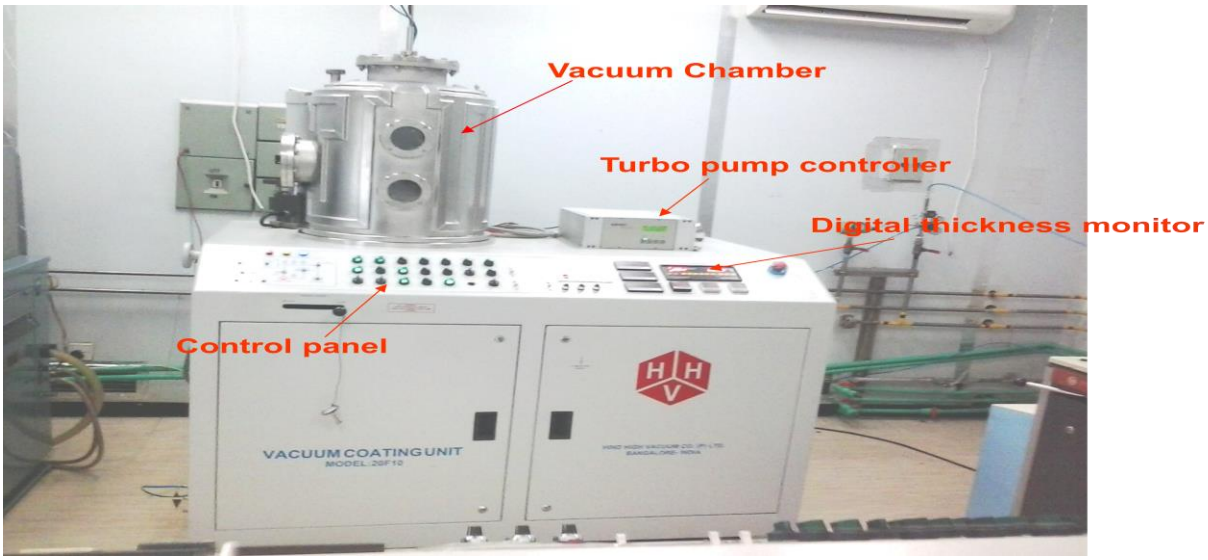

Figure 3.1 : Thermal(vacuum) evaporation system

Figure 3.2 :inside view of thermal evaporation system

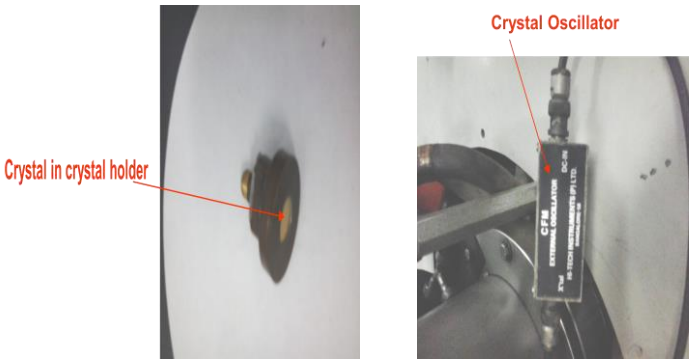

Figure 3.3:quartz crystal & oscillator

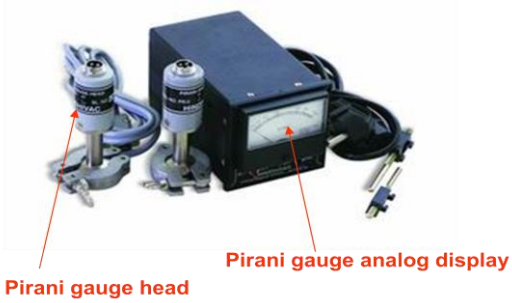

Figure 3.4: Pirani Gauge

Figure 3.5: Penning Gauge

Thermal evaporation system consists of multi turret to resistively heat molybdenum boat or tungsten filament/basket into source material (gold, tin or indium) is kept, radiant heater, quartz crystal assembly as shown in figure 3.2. To measure the film thickness during process as well as rate of deposition, it consists of digital thickness monitor (DTM) which is basically a piezoelectric transducer. It consists of quartz crystal of standard 6MHz frequency with crystal assembly and digital monitor as shown in figure 3.3. This frequency of crystal decreases with damped oscillation during deposition with time and for this crystal oscillator is attached with crystal assembly as shown in figure 3.3. This quartz crystal needs regular cleaning with certain chemical depending upon the evaporant (source) material. Furthur this thickness of deposited film can be measured with dektek surface profilometer. To measure the rotary pump and turbo molecular pump vacuum thermal evaporation system consists of pirani gauge and penning gauge with gauge head as shown in figure 3.4 & 3.5. For initial pre-heating of source material (gold, tin or indium) to remove oxides etc a source shutter is provided in the system. A liquid nitrogen trap is provided inside the thermal evaporation of system to get more fine and fast vacuum in the system as well as acts as a barrier in oil diffusion pump for hot oil vapor not going into the vacuum chamber. Sometimes high discharge Ar gas plasma substrate cleaning can be done at vacuum of 5×10^{-3} mbar, if needed. The films were deposited on the silicon substrates cleaned in the ultrasound bath in isopropyl alcohol and drained by a compressed air flux. During the deposition, all substrates were kept at room temperature i.e no substrate heating or cooling. Gold, Tin and Indium films were evaporated at residual vacuum from molybdenum boat at temperature of 2000°K, 1855˚K. and 1650˚K respectively. Deposition was provided up to full evaporation of material from the molybdenum boat. Portions of the material for evaporation were prepared with help of the microbalance ViBRA. Value of this mass was found by calculation from the defined (nominal) film thickness using follows relation written for the point evaporation source:

$$t = M \cos\theta / 4 \pi \rho r^2$$

where t is the nominal film thickness,

M is the mass of the evaporated material,

ρ is the material density,

r is the distance between an evaporation source and a substrate, and

θ is the deposition angle defined by geometry of the substrate.

It should be noted, that this formula can be used only for rough estimation of an average thickness of ultra-thin films. In this case, certain assumptions about the structure of the film, the shape and size of the islands, can be made only on the basis of measurement of electrical and optical properties of this film and topographic surveillance using XRD, SEM or AFM. Optical absorption and transmittance of gold, tin & indium films on glass substrates were measured in wavelength range from 200 to 1100 nm using the 640FT IR spectrometer. Flow regimes are categorized quantitatively via the Knudsen number (Kn), which represents the ratio of the molecular mean free path to the flow geometry size for gases:

Table 1: different flow resigms

Flow type	**Knudsen Number**
Continuum flow	Kn<0.01
Slip flow	0.01<Kn<0.1
Transitional flow	0.1<Kn<10
Free molecular flow	Kn>10

Vapor pressure varies depending upon the source temperature and is different for different materials, for suitability standard plot [31] is provided from which depending upon source material vapor pressure is selected.

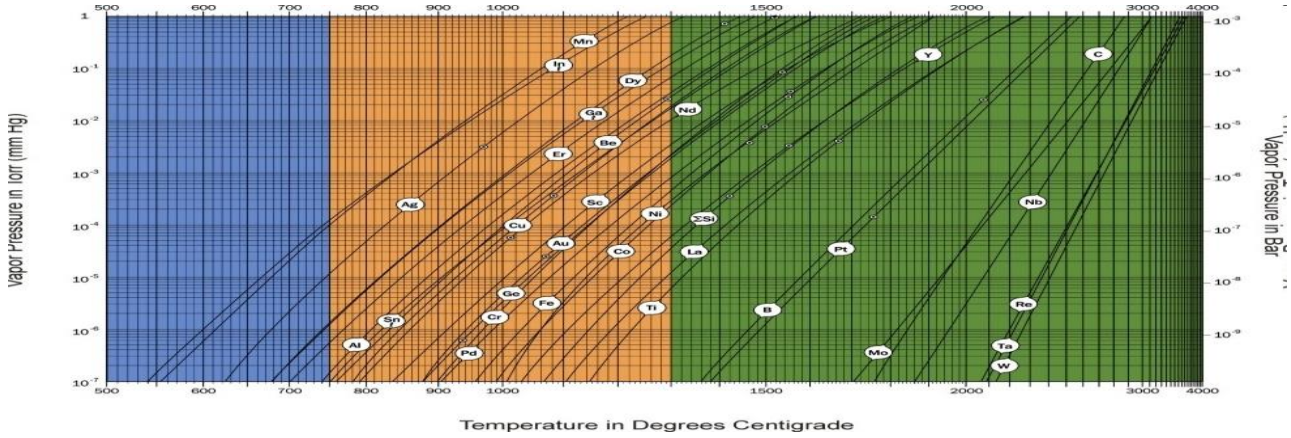

Figure 3.6 : graph between vapour pressures of source Vs temperature [31]

Chapter 4

MODEL DESCRIPTION & FORMULATION

4.1 Model Description

General description of the model is presented in fig. 4.1 where pressure gas flow low in vacuum system i.e molecular flow and it can be seen that the model inputs are ambient temperature, evaporant temperature, vapor pressure, molecular weight, density of gold, neglecting the substrate surface temperature. The Free Molecular Flow interface uses the angular coefficient method to model flows with Knudsen numbers Kn >10. This physics interface avoids solving the physics in the volumes of the modeled geometries, and requires meshing only of the surfaces. Completely diffuse scattering (total accommodation) and emission are assumed at all surfaces in the geometry, and flow is computed by integrating the flux arriving at a surface from all other surfaces in its line-of-sight. This means that the dependent variables exist only on the surfaces of the geometry, and the solution process is much faster than the DSMC method. Furthermore, it is not subject to statistical scatter. Number densities are reconstructed using a method included in the Free Molecular Flow interface. The Molecular Flow Module is designed to offer previously unavailable simulation capabilities for the accurate modeling of low pressure, low velocity gas flows in complex geometries. It is ideal for the simulation of vacuum systems including those used in semiconductor processing, particle accelerators and mass spectrometers. Small channel applications (e.g. shale gas exploration and flow in nanoporous materials) can also be addressed. The Molecular Flow Module uses a fast angular coefficient method to simulate steady-state free molecular flows. We can model isothermal and non-isothermal molecular flows, and automatically calculate the heat flux contribution from the gas molecules. The discrete velocity method is also included in the module for the simulation of transitional flows. Historically, flows in this regime have been modeled by the direct simulation Monte Carlo (DSMC) method. This computes the trajectories of large numbers of randomized particles through the system, but introduces statistical noise to the modeling process. For low velocity flows, such as those encountered in vacuum systems, the noise introduced by DSMC renders the simulations unfeasible. COMSOL uses alternative approaches: employing a discrete velocity method for transitional flows (using a Lattice Boltzmann velocity quadrature) and the angular coefficient method for molecular flows. Using the input parameters, the model computes the thickness of gold deposited, mass deposited on the surface of substrate, mass transfer rate and mass loss by using COMSOL software. The following wall conditions are inbuilt in COMSOL software:

- wall
- outgassing wall
- adsorption/desorption
- deposition

In adsorption/desorption boundry condition, sticking coefficient can be defined along with other condition. Gold, tin and indium is placed in resistively heated tungstun/molybdenum boat which is having very high melting point of 3420^{o}C. Substrate is one quarter of a 4″ wafer mounted on stationary support on top of tungsten boat depending upon the mean free path and Langumuire-Kundsen relation. A screen is placed to cover the substrate, if more than one source is used.

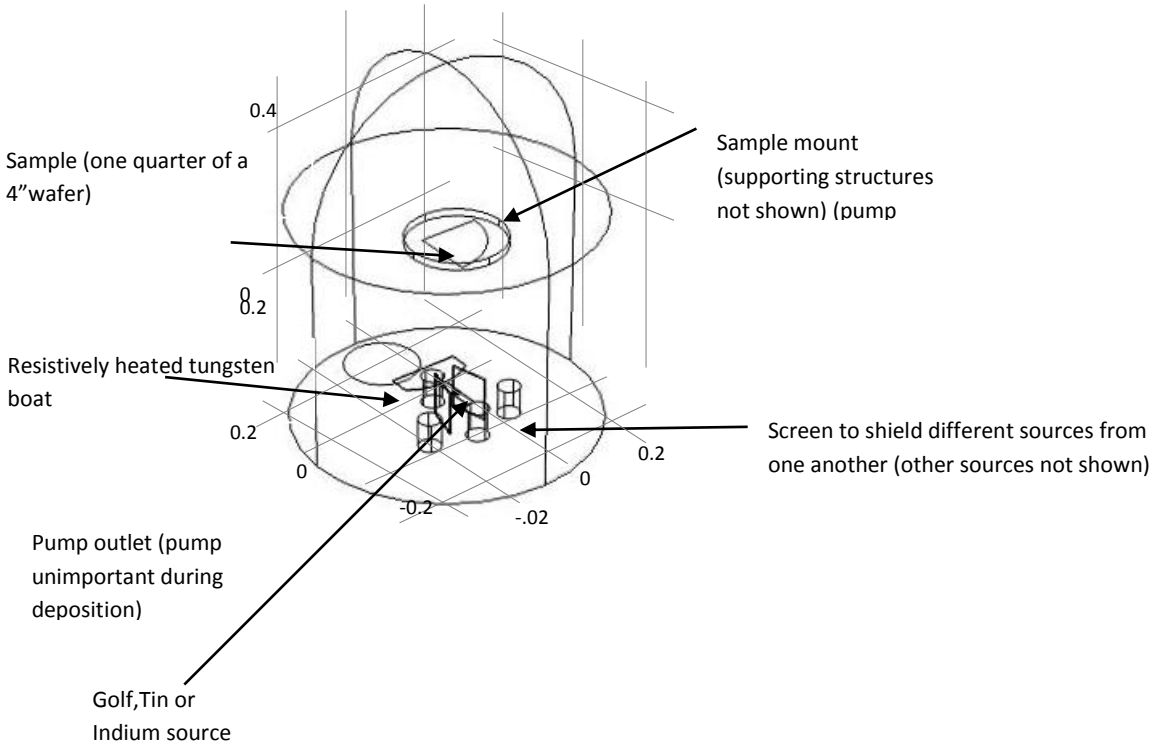

Figure 4.1 : Model Geometry Various components of evaporator

4.2 Model Interfaces :

In the free molecular flow regime, the mean free path of a gas is larger than the dimensions of the object being considered. Equivalently the Knudsen number is much greater than 1. Gas molecules therefore interact with surfaces more frequently than they interact with one another and the flow of gas is determined by collisions with the surfaces in the system.

The Free Molecular Flow (fmf) interface, found under the Rarefied Flow branch is intended for molecular flow interacting with objects that are moving slowly with respect to the speed of the molecules, such as vacuum systems. Diffuse reflection from all surfaces is assumed (this is reasonable in the majority of practical situations) with molecules from all directions effectively adsorbed onto the surface and subsequently re-emitted according to Knudsen's law (i.e. with an intensity that varies as the cosine of the angle of emission to the normal to the surface). For this physics interface the transient solver computes a quasi-static flow.

When this physics interface is added, these default nodes are also added to the **Model Builder**- **Molecular Flow**, **Wall**, and **Initial Values**. Then, from the Physics toolbar, added other nodes that implement e.g. boundary conditions and volume forces. The Free Molecular Flow Interface has following domain, boundary, edge, point and pair nodes :

Number Density Reconstruction

Used the Number Density Reconstruction node to compute the number density on interior domains, boundaries, edges or points at the time of solving the model. In addition to the Number Density Reconstruction features the Free Molecular Flow interface also includes an operator that can be used in postprocessing or in the absence of geometry elements to select. The number density operator is called in the following manner :

comp1.fmf.nop_name(x,y,z)	(in 3D)
comp1.fmf.nop_name(x,y)	(in 2D)
comp1.fmf.nop_name(r,z)	(in 2D axisymmetric)

where name is the dependent variable name for a given species. The default is G, so comp1.nop_G(x,y,z) would be the default operator to compute the number density in 3D. If there are multiple components or Free Molecular Flow interfaces in the model, change the component Name comp1 and physics interface Name fmf accordingly.

Molecular flow

We used the **Molecular flow** node to define the mean molar mass. This is required to compute the pressure, number density, and heat flux at the boundaries. By default the **Mean molar mass** $M_{n,\,G}$ (in kg/mol) is **user defined**. For each species, enter a value or expression in the field. The default is 0.028 kg/mol.

Surface Temperature

We used the **Surface temperature** node to define the surface temperature at the boundary. For non-isothermal models, additional Surface Temperature features can be added to the model to define different temperatures on different surfaces. The temperature can also be computed by a second coupled physics interface(for example a Heat Transfer in Solids interface). By default the Temperature(in K) is user defined. The default is 293.15 K. If additional physics interfaces (such as a Heat Transfer in Solid interface) are available which compute the temperature, the output of these physics interfaces can be selected.

Evaporation

We used the Evaporation node to define an evaporative source. This feature is usually used in combination with a Surface Temperature node, which sets the temperature of the source. For each species, enter a **Vapor pressure** p_{vap} ,G(in Pascal) for the evaporating material. The default is 0 Pa. For each species, enter an **Evaporation coefficient** α_v ,G (dimensionless) for the evaporating material. The default is 1.

Initial Values

The Initial Values node adds initial values for the incident molecular flux, number density, and pressure. For the transient solver, these values define the state of the problem at the initial time step; for the stationary solver, they serve as a starting point for the nonlinear solver.

For transient problems it is often difficult to specify consistent initial conditions. It is possible to add a stationary step in the study to serve as the initial condition for the transient problem, or to start the system at total vacuum (all values equal to zero) and to ramp up the pressure or flux at inlets or reservoirs prior to adding time-dependent effects.

Incident Molecular flux

For each species, enter the **Incident molecular flux**, G_G ($1/(m^2 sec)$ units).

Pressure

For each species, enter the **pressure**, p_G (in Pascal).

Number Density

For each species, enter the **Number density**, n_G (in $1/m^3$ unit).

Wall

The Wall feature provides boundary conditions for modeling different kinds of solid surfaces within vacuum systems.

Wall Type

Select **Wall type- Wall** (the default), **Outgassing wall**, **Adsorption/desorption**, or **Deposition**. For **Wall** it sets the incoming molecular flux for each species, G, equal to the flux emitted from the wall, J. Therefore all the molecules are diffusely reflected.

Flux

For Outgassing wall it allows an additional outgassing flux $J_{0,G}$ to be added to the incident flux, so the total emitted flux for each species is given by

$$J = G + J_{0,G} .$$

Select an **Outgoing flux-Specify directly** (the default), **Number of SCCM units**, **Mass flux**, **Total mass flow**, or **Thermal desorption rate**.

Specify Directly

For **Specify directly**, and for each species, enter a value or expression for $J_{0,G}$ (in $1/(m^2 sec)$ unit).

Number of SCCM(Standard Cubic Centimeters Per Minute) units

For **Number of SCCM units**, and for each species, enter $Q_{sccm,G}$ (dimensionless). This quantity is automatically converted to a standardized volumetric flow rate in SI units. Select an option from the **Standard flow rate defined by** list-**Standard density** (the default) or **Standard pressure and temperature.**

- For **Standard density** enter a **Standard molar volume** V_m (in m^3 /mol). The default is 0.0224136 m^3/mol (in accordance with SEMI standard E12-0303).
- For **Standard pressure and temperature** enter a **Standard pressure** P_{st} (in Pascal) and **Standard temperature** T_{st} (in K). For 2D components, also enter a **Channel thickness** d_{bc} (in meter).

Mass Flux

For **Mass flux**, and for each species, enter a value or expression for M (in $kg/(m^2.sec)$). The default is 0 $kg/(m^2 sec)$.

Total Mass Flow

For **Total mass flow**, and for each species, enter a value or expression for $Q_{m,G}$ (kg/sec). The default is 0 kg/sec. For 2D components, also enter a **Channel thickness** d_{bc} (in meter). This is used to specify the depth of the boundary in the out-of-plane direction.

Thermal Desorption Rate

For **Thermal desorption rate**, and for each species, enter a value or expression for $D_{r,G}$ (in W/m^2). The default is 3e -12 [torr*1/(cm^2*s)]. The outgassing flux, $J_{0,G}$ is related to the thermal desorption rate via

$$J_{0,G} = N_A D_{r,G} / RT$$

, where N_A is Avogadro's number,

R is the universal gas constant and

T is the temperature.

Adsorption/Desorption

For **Adsorption/desorption** it is used in transient models to model adsorption and desorption of gas molecules on the surface. For each of the species enter the following information.

- **Sticking coefficient** S_G (dimensionless). This defines the probability that molecules incident on the surface are adsorbed.
- **Desorption rate** D_G (in mol/(m^2sec)). This defines the rate of desorption. The boundary condition tracks the number of moles of adsorbed per unit area of the surface(fmf.n_ads) as a function of time.
- **Initial adsorbent concentration** $n_{ads,0,G}$ (in mol/ m^2)
- **Additional molar flux** Γ_G (in mol/(m^2sec)) can be added to the surface, enabling, for example , the modeling of molecules arriving at the surface by diffusion through the walls of the chamber from the outside (these molecules are added to the adsorbed molecules on he surface).

Note that molar units are used for the adsorbed molecules, but the total number of molecules per unit are is available as the variable fmf.N_ads.

Solving for the adsorbent concentration can cause convergence issues if the concentration is close to zero, as its value can sometimes go negative during the solution process. If this happens when using this boundary condition, tighten the relative solver tolevance(see the settings for the **Study I> Time-Dependent /solver** node) to 1e-3. Then in the settings for the **Study I > solver configurations>Time-Dependent Solver** node change the absolute tolerance to 1e-4 (if this node is not visible right-click the **Study I** node and select **Show Default solver**).

Deposition

Deposition is used for simulations in which the molecular flow of a despoited species is tracked. It is assumed that all the molecules arriving at the surface are deposited.

For each species, enter a **Film density** $\rho_{film,\,G}$ (in kg/m^3 unit) and **Initial film thickness** $h_{film,\,0,\,G}$ (in meter) to compute the film thickness(fmf.h_film) as a function of time.

Diffuse Flux

The **Diffuse Flux** boundary condition sets the molecular flux emitted from the boundary to a user-specified value. The flux is emitted according to Knudsen's Law (the emitted flux in a given direction is proportional to the cosine of its angle to the surface normal). This can be set directly as a flux, as total incoming mass flow, or number of SCCMs.

Select the **Outgoing flux-Specify directly** (the default), **Number of SCCM units**, **Mass flux**, or **Total mass flow**. The rest of the settings are the same as for Wall, described in the Flux section.

Total Vacuum

Used the **Total Vacuum** boundary condition to set the flux emitted from the wall, J, equal to zero. This is equivalent to an opening to a large vessel or extended region with a much lower pressure than that in the system.

Reservoir

The **Reservoir** boundary condition computes the incoming molecular flux from a large adjacent vessel or region filled with gas at a specified number density or pressure. In this case the effusing flux obeys Knudsen's Law. The reservoir boundary condition represents an opening to an adjacent chamber whose extent is much larger than eh molecular mean free path. The boundary condition assumes that the molecules int eh reservoir have a Maxwellian distribution of velocities and that the size of the opening to the reservoir is much less than the mean free path. Molecules travel through the opening by a process known as molecular effusion. Effusion is a process that selects molecules with higher molecular speeds than average, because they are travelling towards the hole faster than the other molecules. Effusing molecules therefore have a larger average velocity than the molecules in the adjacent reservoir. As a result the pressure or number density at the reservoir boundary can differ from the value set in the boundary condition- which determines the pressure that would be measured within the reservoir away from the opening.

Reservoir

Select the **Boundary condition-Reservoir pressure** (the default) or **Reservoir number density**.

- For **Reservoir pressure**, and for each species, enter a value or expression for the **Reservoir pressure** $p_{0,G}$ (in Pascal). The default is 0 Pa.
- For **Reservoir number density**, and for each species, enter the **Reservoir number density** $n_{0,G}$ (in $1/m^3$ unit).

Vacuum Pump

Used the **Vacuum Pump** node to represent a vacuum pump such as a turbo molecular pump or a diffusion pump. Select how to **Specify pump flux-Fraction of incident molecules** (the default), **Directly**, or Pumpspeed. The emitted flux J is given by

$$J = G - J_{pump}.$$

The **fraction of incident molecules** f_G, is specified either directly, or through a **Pump speed**, S_G , such that

$$f = \sqrt{(2\pi M_n /RT)}\, S/A$$

where M is the molar mass of the species

R is the universal gas constant

T is the temperature

A is the area of the pump

This condition applies pointwise across the surface of the pump. Also ensured that $J_{pump,G}$ value is never negative.

- For **Directly,** and for each species, enter a value for $J_{pump,G}$ (in mol/ (m^2sec) unit)
- For **Fraction of incident molecules**, and for each species, enter a value for f_G (dimensionless). The default is 0.8.
- For **Pump speed**, and for each species, enter a value or expression for S_G (in m^3/sec). The default is 500 1/s.

For 2D components, also enter a **Channel thickness** d_{bc} (in meter). This specifies the out-of-plane thickness of the pump, which is required in order to compute its area.

4.3 Formulation

Mass & Thickness of a deposit: (ref. [35])

If the material arrives at a small area dS_2 on a surface inclined at an angle θ to the direction of the vapor stream, then we can calculate the thickness and the amount of material deposited on such an area.We have

$$d\omega = \frac{\cos\theta \ . \ dS_2}{r^2}$$

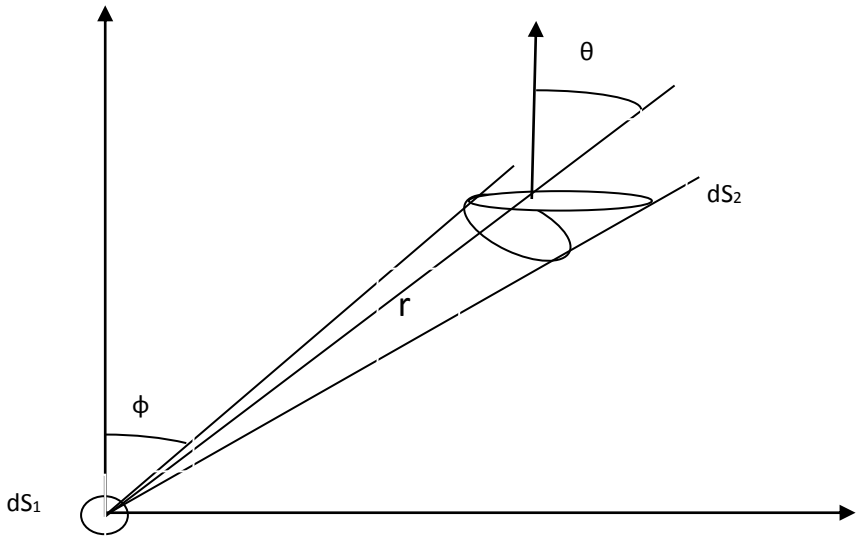

Figure 4.2 : Evaporation of m g/sec from a source S through solid angle dω & receiving surface dS_2 whose normal makes an angle θ with the direction of vapor stream

so the material arrives on dS_2 at the rates

$$dm = \frac{m \cdot \cos\theta \cdot}{4\pi \quad r^2} dS_2 \qquad \text{(in case of point source)}$$

and

$$dm = \frac{m \quad \cos\varphi \quad \cos\theta}{\pi \quad r^2} dS_2 \qquad \text{(in case of surface source)}$$

Suppose the material to be evaporated has a density ρ (g/cm^3), and the thickness of the film condensed per unit time is t (cm/sec), then the volume of material deposited on dS_2 is $t \cdot dS_2$ so that

$$dm = \rho \cdot t.dS_2$$

The thickness of the deposit at points corresponding to the area dS_2 is therefore given by the expression:

$$t = \frac{m \cdot \cos\theta}{4\pi\rho \quad r^2} \qquad \text{(in case of point source)}$$

$$t = \frac{m \quad \cos\theta \ \cos\varphi}{\pi\rho \quad r^2} \qquad \text{(in case of surface source)}$$

The basic governing equation for depositing molecular flux on the surface is Langmuire-Knudsen Relation which shows the **mass deposition rate per unit area of source surface :**

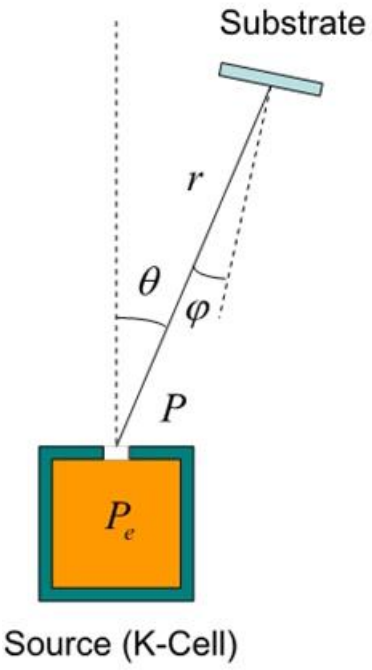

Figure 4.3 : mass deposition rate/unit area of source surface on flat substrate (ref. [22])

$$R_m = C_m \left(\frac{M}{T} \right)^{1/2} \cos\theta \cos\varphi \, (1/r^2) \, (P_e(T) - P)$$

where $C_m = 1.85 \times 10^{-2}$

r = source-substrate distance (cm)

T = source temperature (K)

P_e = evaporant vapor pressure (torr), function of T

P = chamber pressure (torr)

M = evaporant gram-molecular mass (g)

Spherical surface with source on its edge :

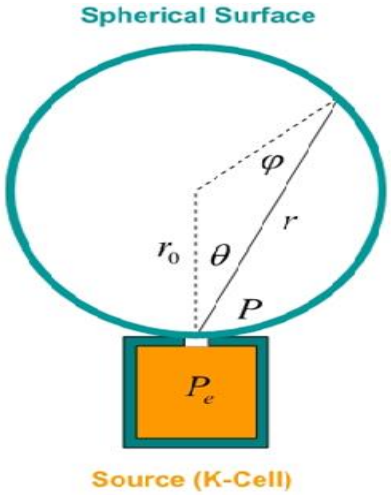

Figure 4.4 : evaporation from source on spherical surface (ref.[22])

$$\text{Cos}\,\theta = \cos\varphi = r / (2 r_0)$$

$$R_m = C_m \left(\frac{M}{T} \right)^{1/2} (P_e / 4 r_0^2)$$

⇨ Angle Independent - uniform coating

⇨ Used to coat instruments with spherical surfaces

Uniformity on a Flat Surface :

Consider the deposition rate difference between wafer center and edge :

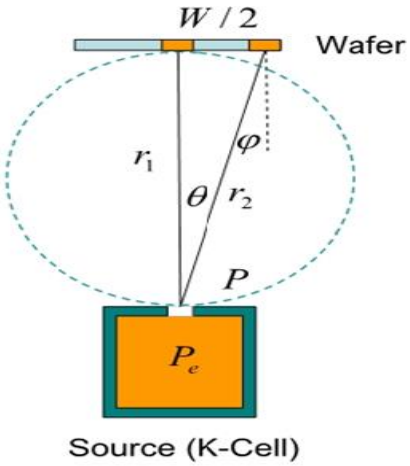

Figure 4.5 : variation of film thickness across the surface of flat substrate (ref. [22])

$$R_1 \propto 1 / r_1^2$$
$$R_2 \propto (1 / r_2^2) \cos^2 \theta = r_1^2 / r_2^4$$

Define Uniformity :

$$\sigma (\%) = (R_1 - R_2) / R_1 \quad (\text{in } \%)$$
$$\sigma = 1 - ((1 + (W / 2r_1)^2)^{-2} \approx W^2 / 2r_1^2$$
$$W / r_1 = \sqrt{(2\sigma)}$$

4.4 Computation of various parameters:

In order to solve a free molecular flow it is always necessary to solve for the incident molecular flux, G for each species. The *Pressure*, *Number density* and *Heat flux* on the surface can be optionally computed by performing additional integrations. The Pressure and Number density are computed by default.

Dependent Variables

Enter the Number of species. The default is 1, but it is possible to add more. It is often convenient to rename the species to something more descriptive for cases when multiple species exist, e.g. H_2 or SiH_4The incident molecular flux G (in $1/(m^2sec)$ dependent variable is always solved for. It represents the incoming flux at the surface (the outgoing flux is available as fmf.J). Other dependent variables might not be solved for, depending on the settings in the **Compute** section.

- The **Pressure** p (in Pascal) represents the total normal force acting on the surface per unit area (including contributions from both incoming and outgoing molecules).
- The **Number density** n (in $1/ (m^3)$), gives the total number density in the vicinity of the surface.
- The **Outward heat flux** Q (in W/m^2) is the heat flux out of the Free Molecular Flow domain as a result of heat adsorbed by the wall as it interacts with the gas.

For each of the dependent variables, the name can be changed in the corresponding field, but the name of fields and dependent variables must be unique within a model.

But in this model pressure & number density are of limited interest so they are not computed in this model.

4.4.1 Computation for Flow :

In many cases it is reasonable to assume that molecules are adsorbed and subsequently diffusely emitted from the surface(or total accommodation). The macroscopic variables in the vicinity of the surface can be derived from kinetic theory. In this instance, the appropriate probability density functions for emission from a surface ($\rho(\theta,c)$ (SI unit : $m^{-1}s$)), have been derived from molecular dynamics simulations [32] and are given by the following equation in 3D:

$$\rho(\theta, c)\sin|\theta|\, d\theta dc = \rho(\theta)\sin|\theta| d\theta d\varphi \,.\, \rho(c)dc \qquad \text{ref. [32]}$$

where θ is the angle to the normal in rad

c is the particle speed in ms^{-1}

with θ in the range

$$-\pi/2 \longrightarrow \pi/2$$

$$0 \longrightarrow \pi$$

The angular and speed probability density functions are given by :

$$\rho(\theta) = (\cos\theta)/\pi$$

$$\rho(c) = (m/k_BT)^2\, c^3/2\, \exp(-mc^2/(2k_BT)) \qquad (4.1)$$

where m is the molecular mass

k_B is the Boltzmann's constant in J/K

T is the temperature in K

c is the speed of the molecules in m/s

permissible value of c is $0 \longrightarrow \infty$

4.4.2 Computation for Particle Flux:

The flux of molecules from x' arriving at point x as shown in figure 4.6 is derived.

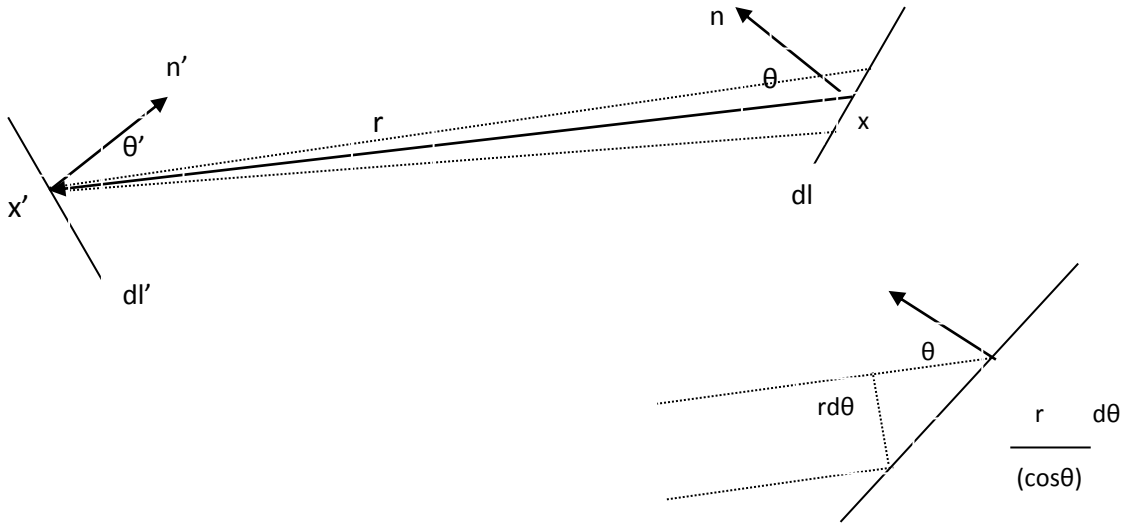

Figure 4.6 : shows the contribution of the flux arriving at point x from point x' in 2 dimensions.

Let the total rate of emission of molecules per unit area at x' be J' in $1/m^2$ s

In the steady state J'is independent of time. In practice the molecules take a finite time to travel from x' to x, but this is not accounted for in the calculations (which are consequently quasi-static).

In 3D, the flux of molecules with speeds between c' and c'+dc' leaving x' with angles between θ' and θ'+ dθ' and φ' + dφ' is

$$J'dS'\rho(\theta')\sin|\theta'|d\theta'd\varphi'.\rho(c')dc'$$

Molecules leaving x' at angles between θ' and θ' +dθ' and φ' + dφ' is spread over an area of

$$r^2 \sin|\theta'|d\theta' d\varphi'$$

in the plane with normal parallel to r at x giving a projected area of

$$(r^2 \sin|\theta'|d\theta' d\varphi') / (\cos \theta)$$

The arriving flux per unit area at x from x', dG (in $m^{-2} s^{-1}$) is, therefore:

$$dG = (J' dS' \cos\theta \rho (\theta') \rho (c')dc') / r^2 \qquad (4.2)$$

The total flux is therefore given by

$$G = \int_S \frac{J'\cos\theta \rho (\theta')}{r^2} dS' \int_0^\infty \rho (c')dc'$$

where the integral is over the surface S' that includes all the surfaces in the line of sight of x.

By the definition of the probability distribution both the integrals over c' evaluate to 1.

Substituting for ρ (θ') the following equations are left:

$$G = \int_S \frac{J'\cos\theta \cos\theta'}{\pi r^2} dS = - \int_S J' \frac{(n.\, r\,)(\, n'.r)}{\pi r^4} dS \qquad (4.3)$$

In the free molecular flow interface, this model computes the incident flux on the surface G as the dependent variable. The outgoing flux from a surface (specified in terms of G by the boundary condition) is also available as fmf.J.

4.4.3 Computation for the Pressure :

The pressure acting on the surface at x can be calculated from the rate of change of momentum of molecules normal to the surface. For incoming molecules the molecules from x' give the following contribution to the pressure on the surface :

$$dp^{in} = \frac{J' dS' \rho(\theta') m \cos^2 \theta\, c' \rho (c')dc'}{r^2}$$

Sustituting for ρ (θ) and integrating gives the total contribution of incoming molecules to the pressure , p^{in} in Pascal, at x :

$$P^{in} = m \int_{S'} \frac{(J'\cos\theta' \cos^2\theta)}{\pi r^2} \int_0^\infty c \rho (c')dc'dS' = \int_{S'} \frac{(J'(n.r)^2 (n'.r)}{\pi r^5} m < c' > dS'$$

From equation no. 4.1 it is shown that :

$$< c' > = \sqrt{(9\pi k_B T) / 8m} \qquad (4.4)$$

The computed incoming pressure contribution is available on surfaces as fmf.Pin

The surface is also emitting molecules at a rate J (in most cases J =G ,but in general this does not need to be the case, for e.g. the surface can be outgassing in addition to emitting the adsorbed molecules so that

$$J = G + J_{out}$$

The emitted molecules also have a normal momentum change that contributes to the pressure in the following manner :

$$dp^{out} = J\, mc \cos\theta\, \rho(\theta)\, \rho(c) \sin|\theta|\, d\varphi\, d\theta\, dc$$

Thus the total pressure contribution from emitted molecules, p^{out} in Pascal is :

$$P^{out} = J\, m \int_{-\frac{\pi}{2}}^{\frac{\pi}{2}} \frac{(\cos^2\theta \sin|\theta|)}{\pi}\, d\theta \int_0^{\pi} 1 d\varphi \left(\int_0^{\infty} c\, \rho(c) d\theta\, dc \right) = \tfrac{2}{3} J\, m < c >$$

substituting for the mean velocity (using equation 3-14 with T' T) the equation obtained :

$$p^{out} = (\pi k_B T\, m / 2)^{1/2} J \qquad (4.5)$$

The outgoing pressure contribution is available in the Free Molecular Flow interface as fmf.Pout.

Finally the total pressure acting on the surface, p in Pascal is given by :

$$p = p_{in} + p_{out}$$

This is computed in the physics interface as the dependent variable p.

4.4.4 Computation for Number Density:

The number density at the surface can also be calculated from a similar argument. Molecules arriving at x from x' with speeds between c and c + dc make a contribution, dn, to the number density, n in 1/ m^3 units , at the surface that is related to their flux at the surface dG by :

$$dn = dG / (c' \cos\theta)$$

Following the same argument, the total incoming number density at x is given by :

$$n^{in} = \int_{S'} \frac{(J' \cos\theta')}{\pi r^2} \int_0^{\infty} \frac{(\rho(c'))}{c} dc' dS' = -\int_{S'} \frac{(J'(n'.r))}{\pi r^3} < \frac{1}{c'} > dS' \qquad (4.6)$$

The mean of inverse speed (calculated using equations 4.1) are given by :

$$< \frac{1}{c'} > = \frac{\sqrt{(\pi m)}}{\sqrt{(8 k_B T)}} \qquad (4.7)$$

The integrand in equation 4.6 depends only on the emitted flux, the normal, and the molecular velocity at the emitting surface (and not on the orientation or properties of the wall where the flux is arriving). Equation 4.6 can therefore be used to compute the flux arriving at any point within the flow domain, in addition to the flux arriving at surfaces. This is the basis of the number density reconstruction features and the number density calculation operator, which can be used to calculate

the number density within the domain.

Considering again the case of a surface in the model, the contribution to the outgoing number density at a given angle and speed the from the emitted molecules is :

$$dn^{out} = \frac{J\,\rho(\theta)\rho(c)\sin|\theta|\,d\varphi\,d\theta\,dc}{c\cos\theta}$$

so the total outgoing number density is given by :

$$n^{out} = J\int_{-\frac{\pi}{2}}^{\frac{\pi}{2}} \frac{(\sin|\theta|)\,d\theta}{\pi} \int_0^{\pi} 1 d\varphi \left(\int_0^{\infty} \frac{\rho(c)\,dc}{c}\right) = 2J\,\langle 1/c\rangle$$

substituting for the mean inverse velocities (using equation 4.7 with $T \longrightarrow T$) the equation obtained

$$n^{out} = (\pi m / 2 k_B T)^{1/2} J$$

The outgoing number density is available in the physics interface as fmf.Nout.

The total number density of the molecules near the surface is therefore:

$$n = n^{in} + n^{out}$$

This is computed in the physics interface as the dependent variable n.

4.4.5 Computation for Heat Flux :

To compute the incident heat flux on a surface it is necessary to sum the kinetic energy of the incident molecule. On average each molecules carries kinetic energy, q_m given by :

$$q_m = \tfrac{1}{2} m \langle c'^2 \rangle$$

equation 4.1 can be used to shown that :

$$\langle c'^2 \rangle = (4k_B T') / m$$

The total kinetic energy arriving at the surface is calculated by multiplying the total flux arriving from a given direction, multiplying this quantity by equation 4.3 , and then integrating over all directions. From equation 4.3 the appropriate integral is given by :

$$Q^{in} = -\int_S \frac{2k_B T}{m} \frac{J'(n \cdot r)(n' \cdot r)}{\pi r^4}\, dS$$

The incoming heat flux is available as fmf.Qin.

The outgoing flux is simply:

$$Q^{out} = \frac{1}{2} m \langle c^2 \rangle J = 2k_B T J$$

The net heat flux removed from the gas is given by :

$$Q^{tot} = Q^{in} - Q^{out}$$

This is the heat flux that flows into the solid walls of the vacuum chamber.
The net heat flux is available as fmf.Qtot.

Boundary Conditions for Pressure and Number Density:

Consider the molecules effused from an infinite half space filled with a gas of number density n through a small hole in the half space with diameter much less than the mean free path of the gas. Within the as the molecules are travelling in all directions on a unit sphere with equal probability. The probability of molecules striking the hole at angles between θ and θ + dθ to the normal of the bounding surface of the half space is proportional to the fraction of solid angle that this angular range occupies.
In 3D, as showin in figure 4.7, the total solid angle corresponding to angles between and θ +dθ and φ and φ+dφ is sin (θ)dθ dφ.

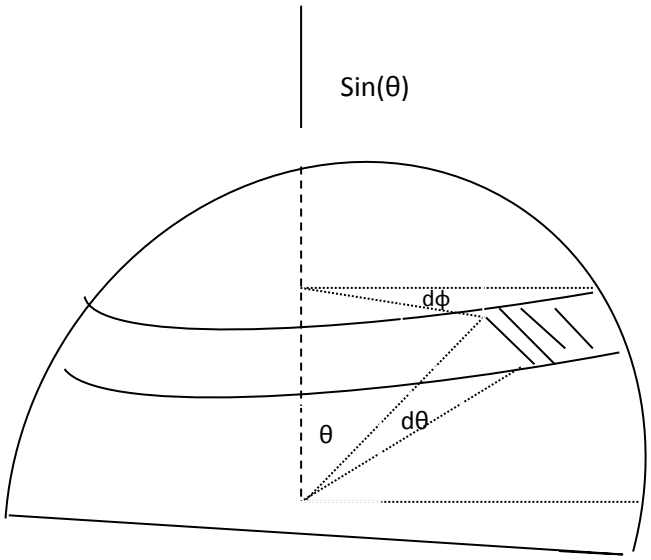

Figure 4.7 : diagram illustrating the portion of solid angles occupied by particles approaching a surface at angles between θ and θ +dθ , and between φ and φ +dφ

The probability of particles effusing at angles between θ +dθ is therefore :

$$\rho^{eff}(c)\, d\theta d\varphi = \frac{1}{4\pi} \sin\theta d\theta d\varphi$$

It is assumed that the molecules are in equilibrium , so their speeds are given by the corresponding Maxwell-Boltzmann distribution in 3D. Therefore :

$$\rho^{eff}(c) = \sqrt{\frac{2}{\pi}} \left(m / (k_B T) \right)^{3/2} c^2 \exp\left(-(mc^2) / 2k_B T \right)$$

If molecules are traveling toward the surface at velocity c then a volume of gas A c cosθ strikes

area A in unit time. The effusing flux contribution is then n c cosθ. The contribution to the total flux from molecules at angles between θ and θ +dθ with speeds c and c +dc is therefore :

$$dJ^{eff} = \frac{1}{4\pi} \sqrt{\frac{2}{\pi}} \left((m)/(k_B T)\right)^{3/2} \cos\theta \sin\theta d\theta d\varphi . c^3 \exp(- (mc^2)/ (2k_B T)) dc \qquad (4.9)$$

Compared this expression to the outgoing flux from a wall , noting that the form of the velocity distribution functions is similar to those in equation 4.1 :

$$dJ^{out} = \frac{1}{2\pi} \left(m / (k_B T)\right)^2 J \cos\theta \sin\theta \, d\theta \, d\varphi \, .c^3 \exp(- (mc^2) / (2k_B T)) dc$$

Therefore, treat the flux effusing into the domain from the half space as a boundary with a flux J^{eff} given by :

$$J^{eff} = \left(\left(k_B T\right) / (2\pi m) \right)^{1/2} n$$

Because the half space is infinite the pressure in this region can still be determined by the ideal gas law giving the following result for the flux at an external pressure , p:

$$J^{eff} = \left((1) / (2\pi m k_B T)\right)^{1/2} p$$

Inverting this expression gives :

$$P = (2\pi m k_B T))^{1/2} J^{eff}$$

Which can be compared with equation 4.5

$$p^{out} = (\pi m k_B T/2))^{1/2} J^{eff}$$

The factor of two difference occurs because the incoming pressure contribution is calculated separately in the case of equation 4.5

Adsorption and Desorption :

There is considerable complexity in the detailed physics of gas adsorption and desorption [33] Some of this complexity is summarized in figure 7, which shows some of the processes involved in the adsorption and desorption of an imaginary diatomic molecule. Molecules incident on a wall of the vacuum system are either reflected or adsorbed. The sticking coefficient defines the probability that an incident molecule is adsorbed. The molecule is usually physically adsorbed initially, being bound to the surface by weak Vander Walls interactions between the adsorbate and the atoms in the solid surface, or in the case of multiple physically adsorbed layers, between the adsorbate and the underlying layer of adsorbed molecules. Molecules adjacent to the surface can then dissociate and chemically adsorb on the metal surface of the chamber. The reverse processes: chemical desorption, followed by re-association can increase the number of physically adsorbed molecules on the surface. These physically adsorbed molecules can dissociate from the surface and consequently contribute ot the desorbed flux. In addition to these processes, gases can pass through the walls of a vacuum system by the process of diffusion.

Depending on the method of manufacturing, a newly constructed vacuum system contains a certain amount of dissolved gas I its walls. Initially the concentration profile of the gases is probably

uniform through the thickness of the wall. When the chamber is pumped out, over a long period of time this uniform concentration changes to a roughly linear profile with a high concentration on the outside and a low concentration on the inside. It takes some time for this concentration profile to develop and the process of reaching this point is frequently referred to as diffusion in the vacuum literature. Once an equilibrium profile is reached then a constant mass transport occurs along the concentration gradient.

This is known as permeation (although the process itself is, of diffusive). Permeation needs to account for the adsorption of the molecules onto the exterior surfaces of the vacuum chamber and the desorption of the molecules from the interior of the chamber.

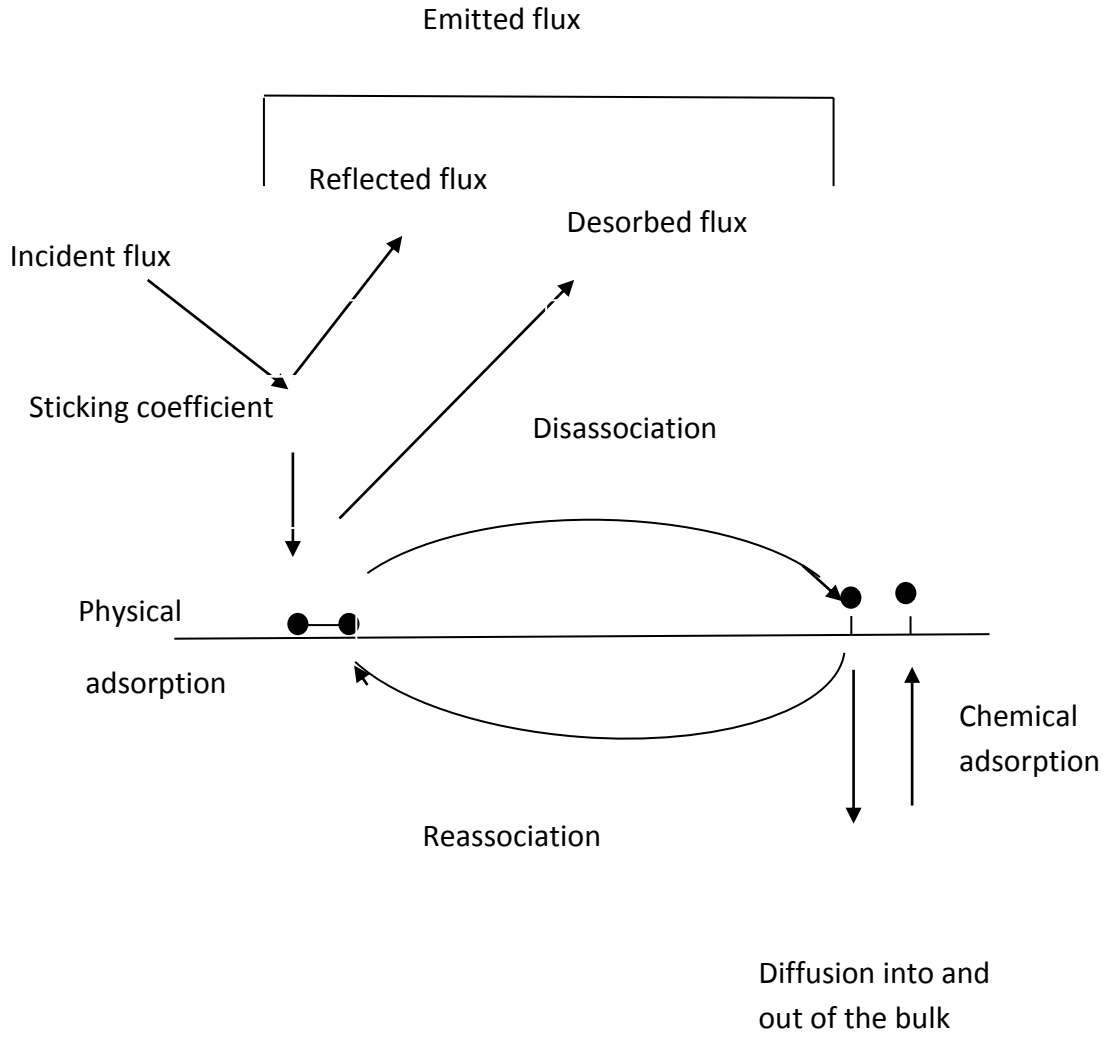

Figure 4.8 : process involved in the adsorption of an imaginary diatomic molecule. It is difficult to obtain the details of the individual reaction processes involved in this process for particular molecules.

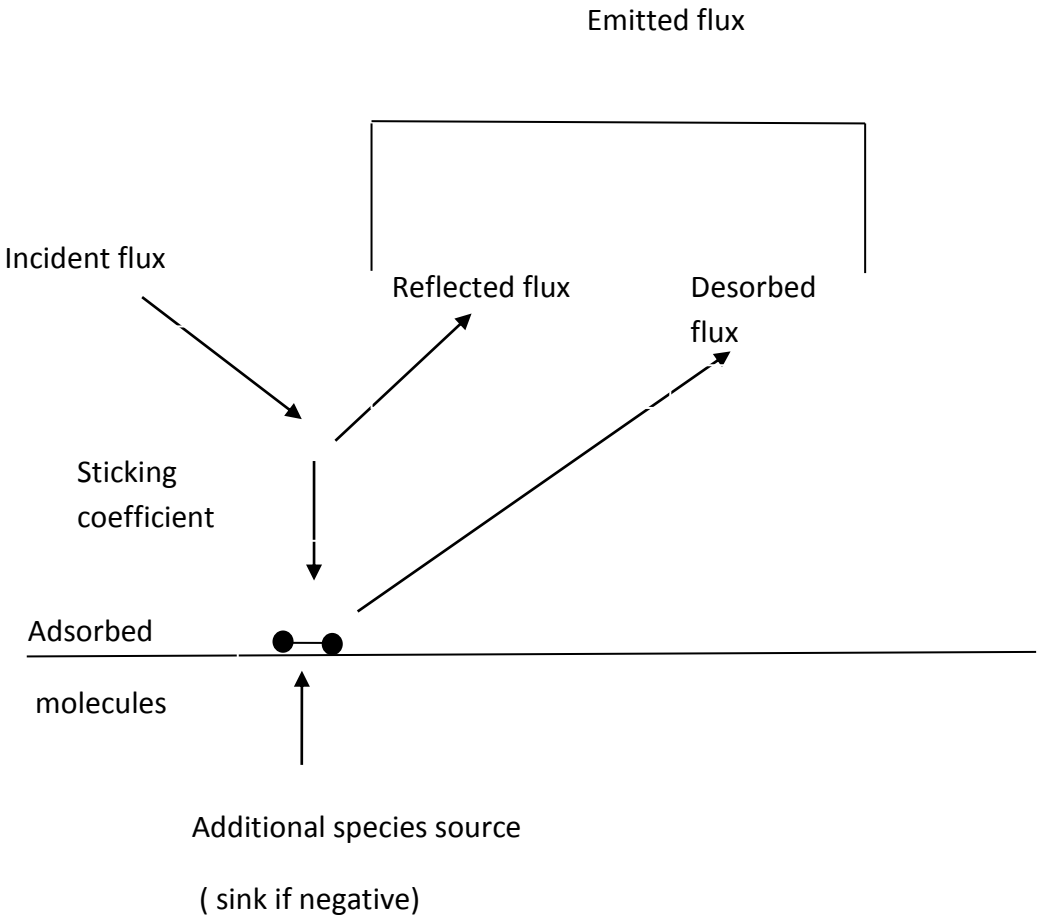

Figure 4.9 : The molecular flow module's simplified adsorption/ desorption scheme. This scheme assumes that the molecule is adsorbed as a whole. Although this might not be physically what is happening the effect of the dissociation can still be added to the model by appropriate modification of the sticking coefficient and the desorption rate.

Modeling the adsorption and desorption of molecules on the surface of a vacuum chamber at this level of detail is possible if the Free Molecular Flow interface is coupled with the Chemical Reaction Engineering Module's Surface Reactions interface. However, in practice there is usually insufficient data available to fully characterize the reactions occurring on the surface of the chamber. Furthermore, the barriers to desorption of physically adsorbed species are small at room temperature, so physical adsorption has little effect on molecular transport in the vacuum system [34]. It is therefore usually appropriate to consider only chemical adsorption. Given these considerations, the Adsorption/Desorption feature considers only the chemical adsorption of the molecule as a whole as shown in fig 8. If the molecule dissociates on adsorption then it is still possible to use this mechanism for practical modeling, but allowance must be made for the fact that the boundary condition tracks the total number of moles of the original gas molecule that have been adsorbed (e.g. of the diatomic molecule the number of moles of the adsorbed species is double this number). An additional source term for the number of adsorbed molecules can be used to include

the effects of diffusion and permeation throught the chamber walls. Very complex and realistic situations can be modeled with this approach.

The adsorption / desorption boundary condition specifies outgoing flux and the number of adsorbed molecules in the following manner :

$$J = (1 - S)G + DN_A$$

$$dn_{ads} / dt = S\frac{G}{NA} - D + \Gamma$$

where J is the emitted molecular flux in molecules /m ^{2}/s

S is the sticking coefficient

G is the incident molecular flux in molecules/m^2/s

N_A is Avagadro's number

n_{ads} is the number of adsorbed moles in mol/m^2

D is the desorption rate in mol/ m^2/s

Γ is the additional source term for the adsorbed molecules in mol/m^2/s

S,D and Γ along with an initial value for the number of adsorbed molecules (n_{ads} ,0), are specified in the boundary condition. These values can be specified as arbitrary functions of the concentration of adsorbed species (fmf.n_ads) allowing for highly flexible modeling of the adsorption and desorption process.

4.4.6 Computation for Evaporation :

The Evaporation boundary condition specifies the outgoing flux using the following expression :

$$J = \alpha_v \ (N_A^2 / 2\pi M_n RT)^{1/2} p_{vap}$$

where α_v is evaporation coefficient as dimensionless parameter

p_{vap} is the vapor pressure in Pascal

N_A is Avagadro's number

M_n is the molecular weight in kg /mol

R is universal gas constant in J/ mol °K

T is the surface temperature in °K

Chapter 5

RESULTS & DISCUSSION

In table 2 various input parameter required for the gold model are given to compute the molecular flow in vacuum system. Generally, the ambient temperature is fixed based on the experimental setup or experimental conditions but the evaporation temperature can be varied as per the thickness or mass transfer to be deposited on the substrate. This evaporation temperature can be increased or decreased considering the vapor pressure, to make fast the mass transfer keeping the good adhesion with uniformity on the substrate surface.

Table 2: Input parameter for the gold model

Name	Expression	Value	Description
Tamb	293.15[K]	293.2 K	Ambient temperature
Tevap	2000[K]	2000 K	Evaporation temperature
pvap	50[Pa]	50.00 Pa	Vapor pressure of gold
Mn0	197[g/mol]	0.1970 kg/mol	Molecular weight of gold
Rho0	19.3 gc/m^3	1.930E4 kg/m³	Density of Gold

Figure 5.1 shows the flux of gold molecules on the surfaces of the model. This constant flux determines the thickness of gold deposited shown in figure 5.2. In figure 5.2, it is obvious the film thickness is maximum in the centre of substrate positioned directly on vertically centre of tungsten boat/source, greater than 38.5 nm after 60 seconds of thermal evaporation process. This thickness decreases radialy outwards surface of the substrate 34.28 nm.

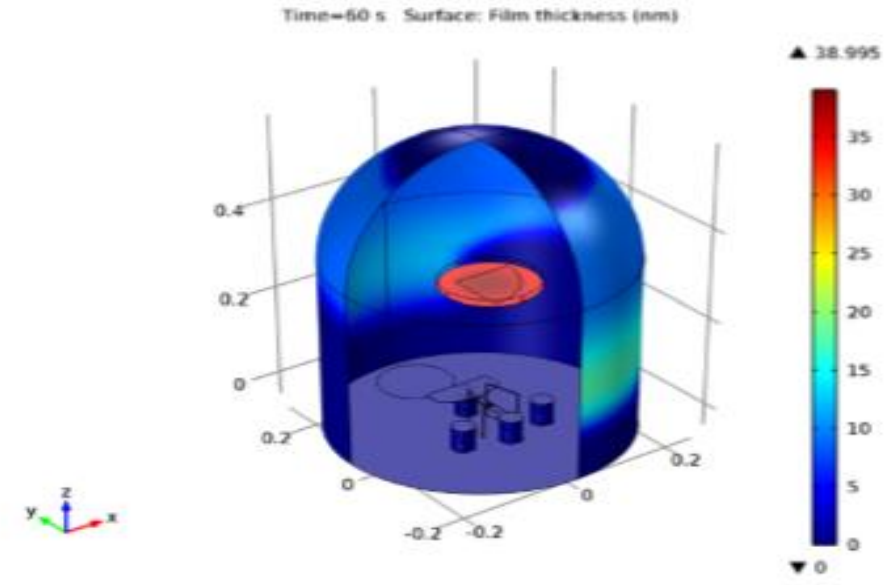

Figure 5.1 : gold film thickness on the surface of system, after 60 sec of deposition

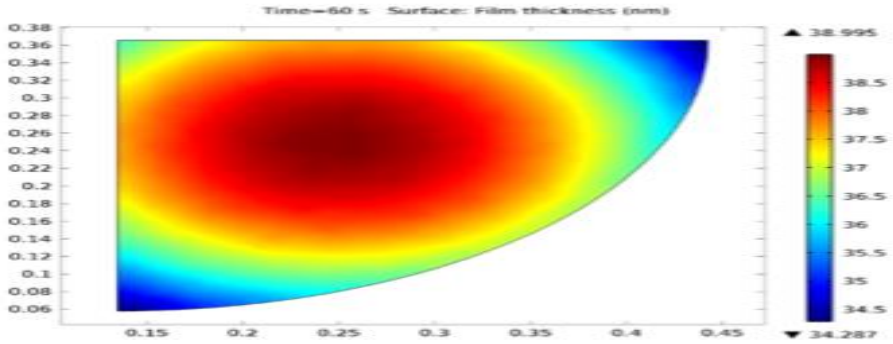

Figure 5.2 : gold film thickness on the sample, after 60 sec of deposition

In figure5.3 based the molecular flux deposited on substrate , graph shows the gold deposited thickness after 60 seconds from initial condition of zero second. It is clear from graph that the film thickness varies linearly with time.

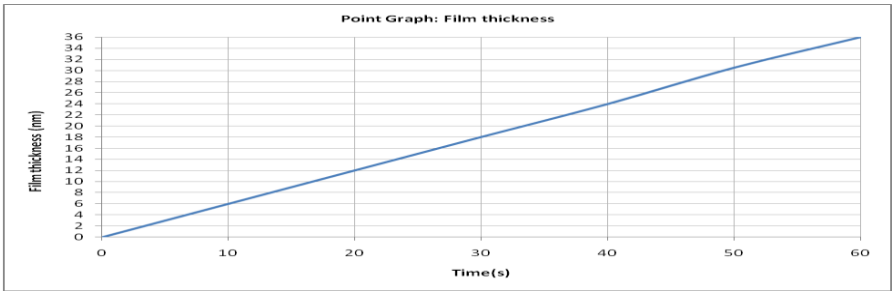

Figure 5.3 : time dependent variation of gold film thickness

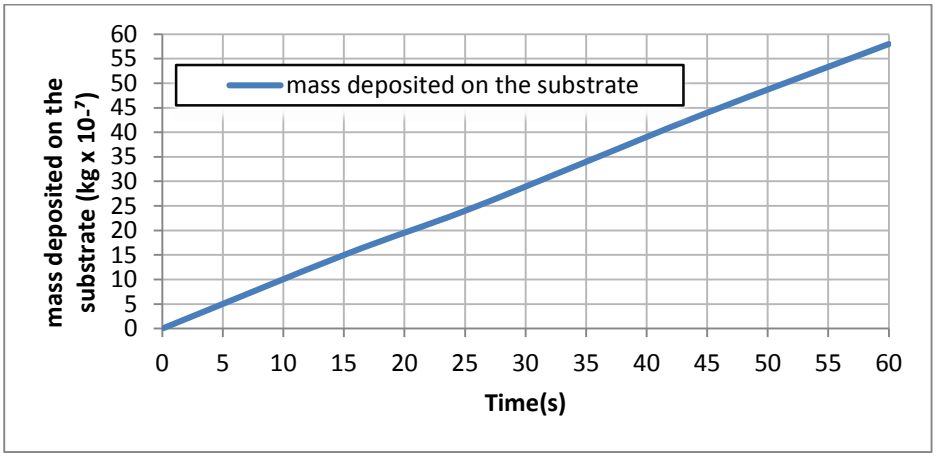

Figure 5.4 : time dependent variation of mass deposited on the substrate with time (60sec)

In figure 5.4 graph is plotted with time for mass (kg x 10^{-7}) deposited on the surface of substrate and shows that as mass deposited on substrate increases with time as in the case of figure 5.3 since the depositing thickness with time adds mass also on the substrate. In figure 5.5 mass transfer rate (kg/sec x 10^{-8}) is plotted for 60 seconds and is a straight constant abscissa parallel line.

Only the flux is required to compute the deposition rate, but in this instance, since most of the computational time is used to compute the view factors, solving the time dependent problem adds little additional time to the solution process. Using a time dependent model also allows for more advanced extensions of the model, for example, re-evaporation of gold from hot surface close to the evaporative source could be included.

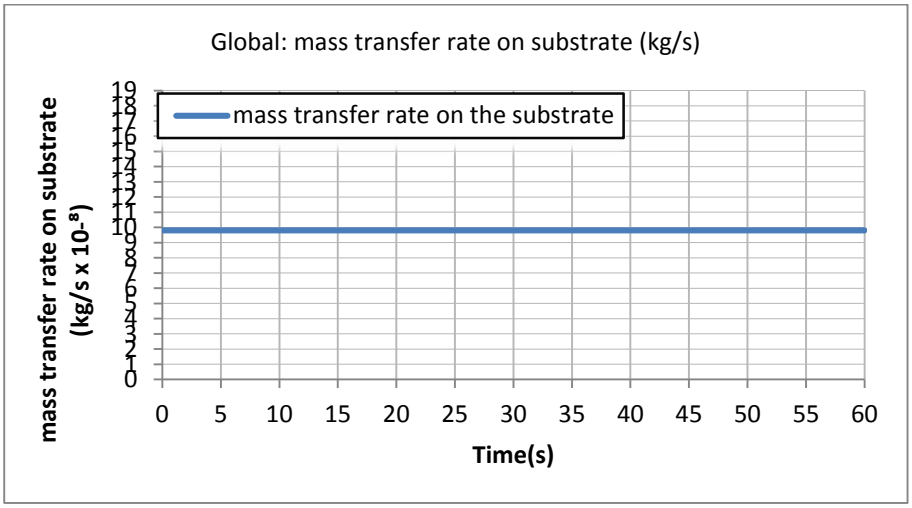

Figure 5.5: mass transfer rate of gold

In table 3 &4 various input parameters required for the Tin and Indium models are given to compute the molecular flow in vacuum system. Generally, the ambient temperature is fixed based on the experimental setup or experimental conditions but the evaporation temperature can be varied as per the thickness or mass transfer to be deposited on the substrate. This evaporation temperature can be increased or decreased depending considering the vapor pressure, to make fast the mass

transfer keeping the good adhesion with uniformity on the substrate surface.

Table 3: Input parameter for the Tin model

Name	Expression	Value	Description
Tamb	293.15[K]	293.2 K	Ambient temperature
Tevap	1855[K]	1855 K	Evaporation temperature
pvap	100[Pa]	50.00 Pa	Vapor pressure of Tin
Mn0	118.71[g/mol]	0.11871kg/mol	Molecular weight of Tin
Rho0	7.36 gc/m^3	7.36E3 kg/m³	Density of Tin

Table 4: Input parameters for the Indium model

Name	Expression	Value	Description
Tamb	293.15[K]	293.2 K	Ambient temperature
Tevap	1485 [K]	2000 K	Evaporation temperature
pvap	100[Pa]	50.00 Pa	Vapor pressure of indium
Mn0	114.818[g/mol]	0.1970 kg/mol	Molecular weight of indium
Rho0	7.31 gc/m^3	1.930E4 kg/m³	Density of indium

Figure 5.6 shows the flux of tin molecules on the surfaces of the model. This constant flux determines the thickness of tin deposited as shown in figure 5.7.From figure 5.7 , it is obvious the tin film thickness is maximum in the centre of substrate positioned directly on vertically centre of tungsten boat/source, 165 nm after 60 seconds of thermal evaporation process. This thickness decreases radialy outwards surface of the substrate to 144 nm. In Figure 5.8 based the molecular flux deposited on substrate, graph shows the tin deposited thickness after 60 seconds from initial condition of zero second. It is clear from graph that the film thickness varies linearly with time.. In figure 5.9 graph is plotted with time for mass (kg x 10^{-6}) deposited on the surface of substrate and shows that as mass deposited on substrate increases with time as in the case of figure 5.8 since the depositing thickness with time adds mass also on the substrate. In figure 5.10 mass transfer rate (kg/sec x 10^{-8})is plotted for 60 seconds and is a straight constant abscissa parallel line.

.

Time = 60 Surface Film thickness (nm)

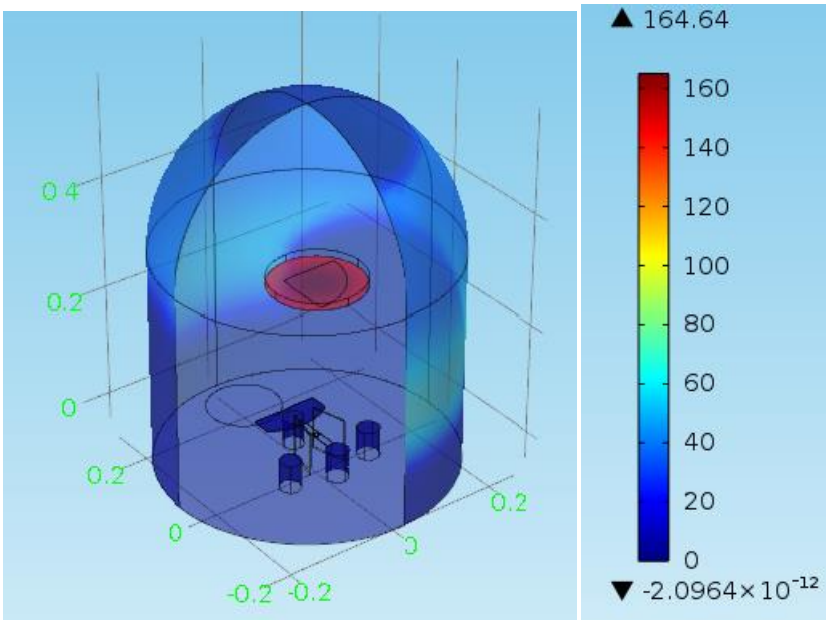

Figure 5.6 : Tin film deposited thickness

Time = 60 sec Surface : film thickness (nm)

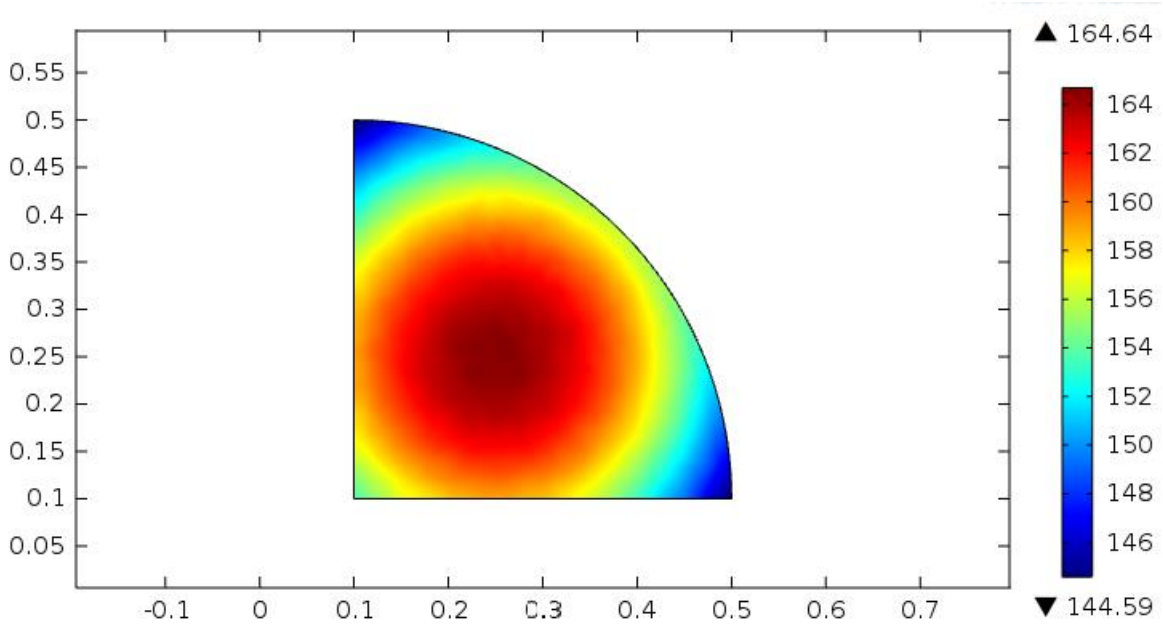

Figure 5.7 : variation of deposited Tin film thickness across the surface

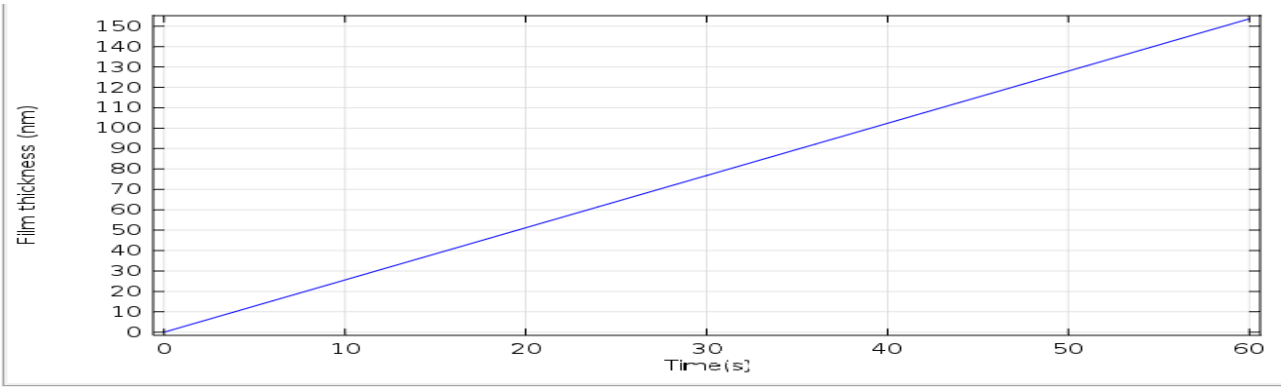

Figure 5.8 : film thickness vs time at a point on the corner of the sample

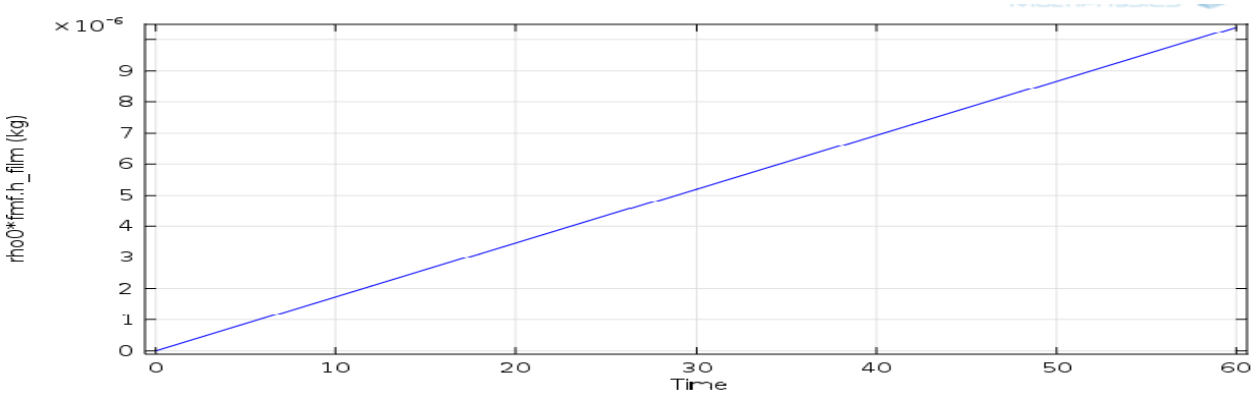

Figure 5.9 : Mass of Tin deposited on the surface

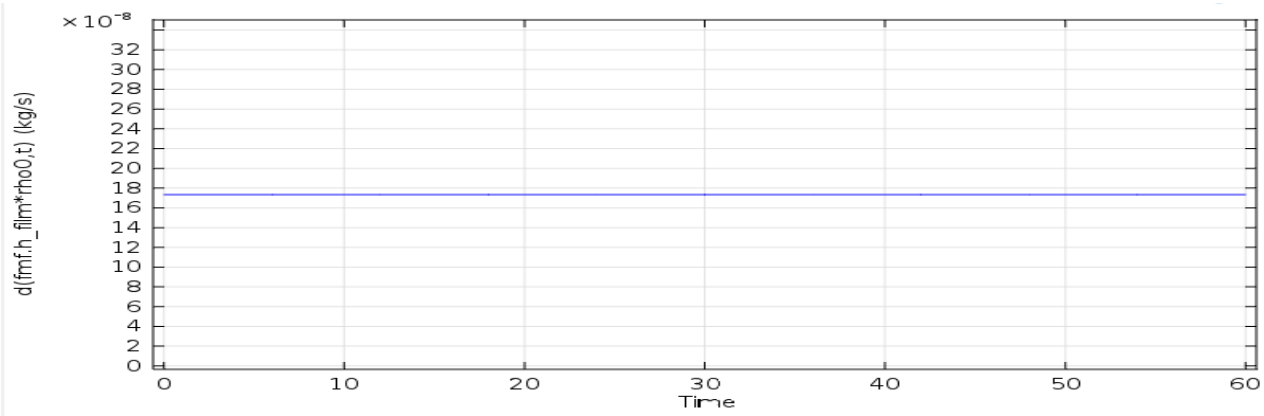

Figure 5.10 : Variation of Mass Transfer rate of Tin with time

Figure 5.11 & figure 5.12 shows the deposition of Indium at 100 Pa with evaporation temperature of 1485 °K. The maximum film thickness achieved is 183 nm; this film thickness may vary by varying the evaporation temperature with time and vapor pressure. Similarly, the Indium thin film thickness varies from 160 to 183nm from the centre of substrate to outer surface and it is maximum at the centre.

Time = 60 sec Surface film thickness (nm)

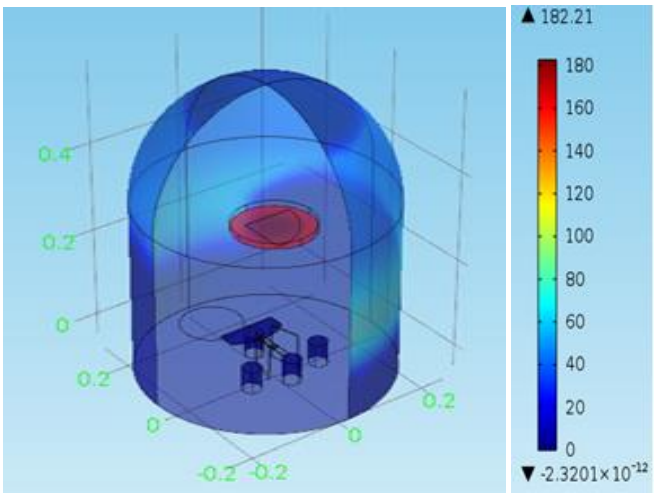

Figure 5.11 : Indium film deposited thickness

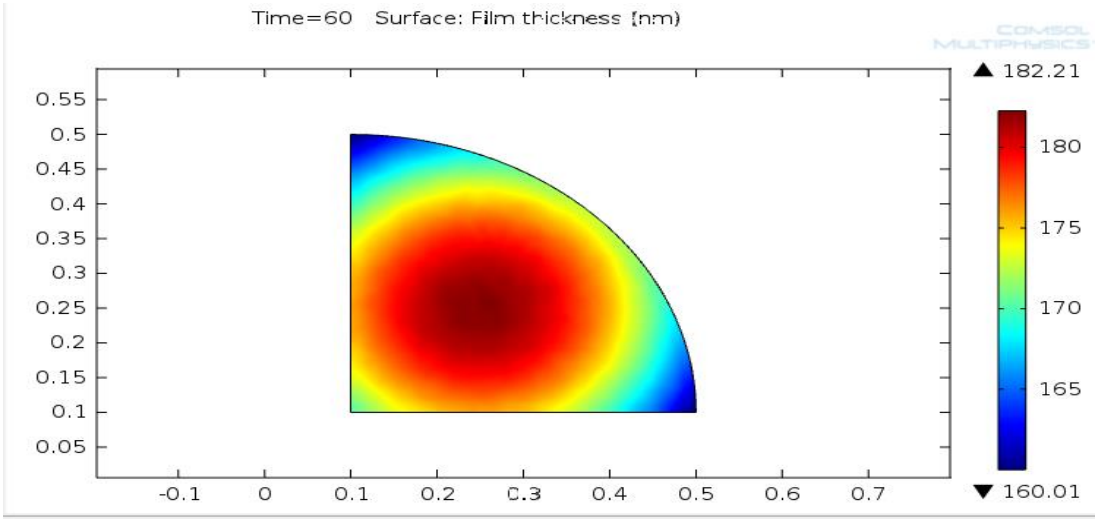

Figure 5.12 : variation of deposited Indium film thickness across the surface

Figure 5.13 shows the variation of thickness at a point on the surface and its variation with time i.e after 60 sec from zero to 183nm. This plot is taken at present at the edge of substrate and similarly by selecting the another point on the surface, we can find similar plot.

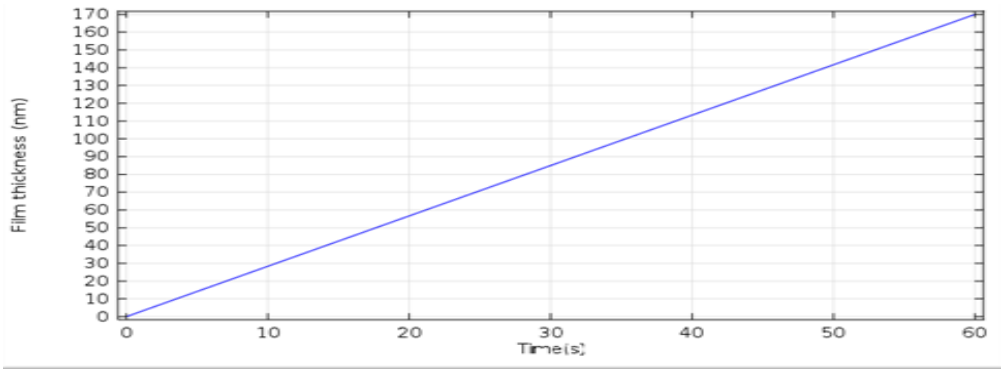

Figure 5.13: film thickness vs time at a point on the corner of the sample

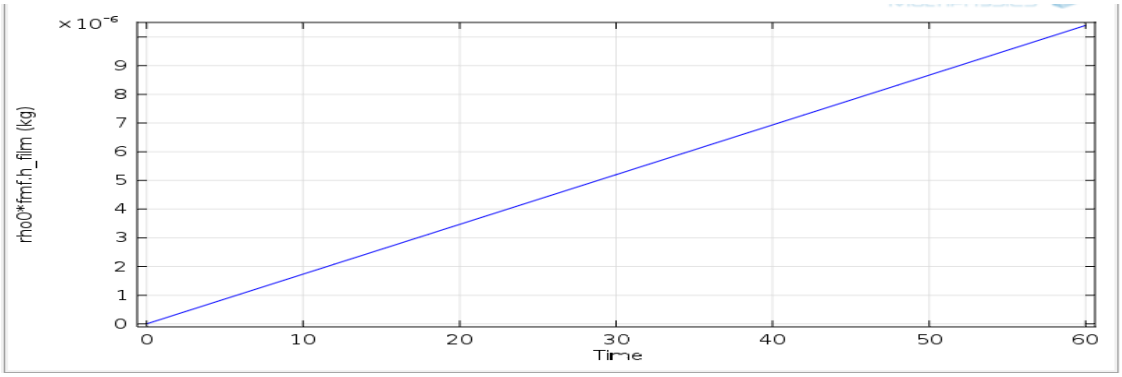

Figure 5.14 : Mass of Indium deposited on the surface

Figure 5.14 shows the mass (kg x E- 6) of indium deposited on the surface of substrate and shows that as mass deposited on substrate increases with time. Now as in the case of figure 5.8 where the depositing thickness with time adds, mass also on the substrate deposited increases.

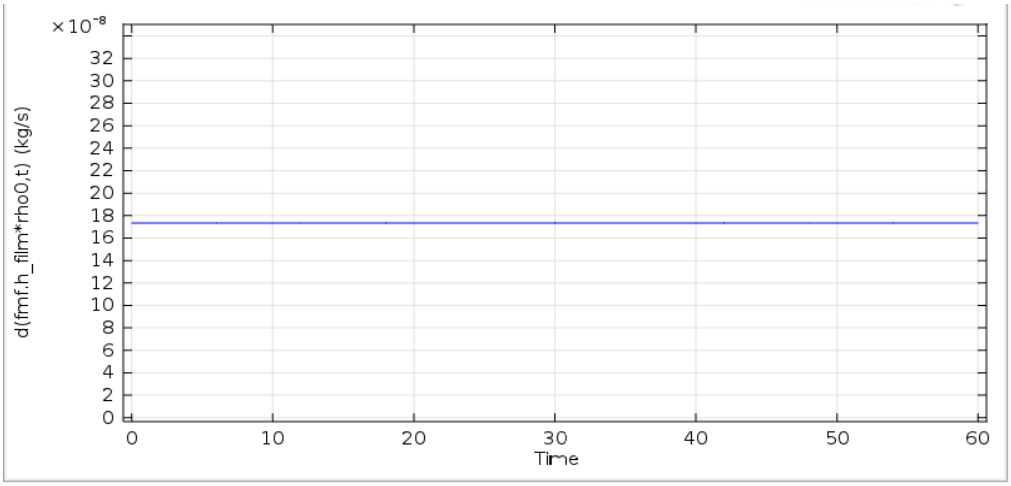

Figure 5.15 : Variation of Mass Transfer Rate of indium with time

Figure 5.15 shows mass transfer rate (kg/sec x 10^{-8}) is plotted for 60 seconds and is a straight constant abscissa parallel line. Only the flux is required to compute the deposition rate, but in this instance, since most of the computational time is used to compute the view factors, solving the time dependent problem adds little additional time to the solution process. Using a time dependent model also allows for more advanced extensions of the model, for example, re-evaporation of gold from hot surface close to the evaporative source could be included. Definitely there is loss of source material during thermal evaporation since only a fraction of the material is deposited on the surface while we are evaporating a large quantity of it. The difference between these two is called mass transfer loss and deposited material is yield from the process.

Figure 5.16 shows that gold SEM micrographs at 5KX , 50KX, 100KX magnification which is very uniform and smooth and average grain size of gold is 12-30nm across the grain boundary.

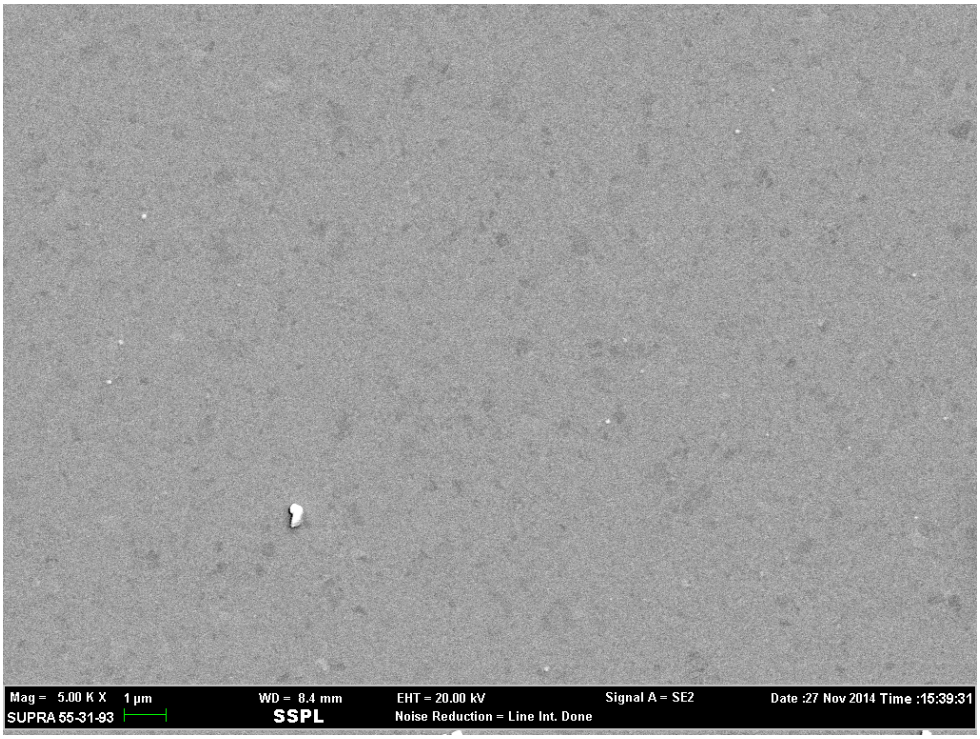

Figure 5.16 : SEM micrograph of gold at 5KX magnification

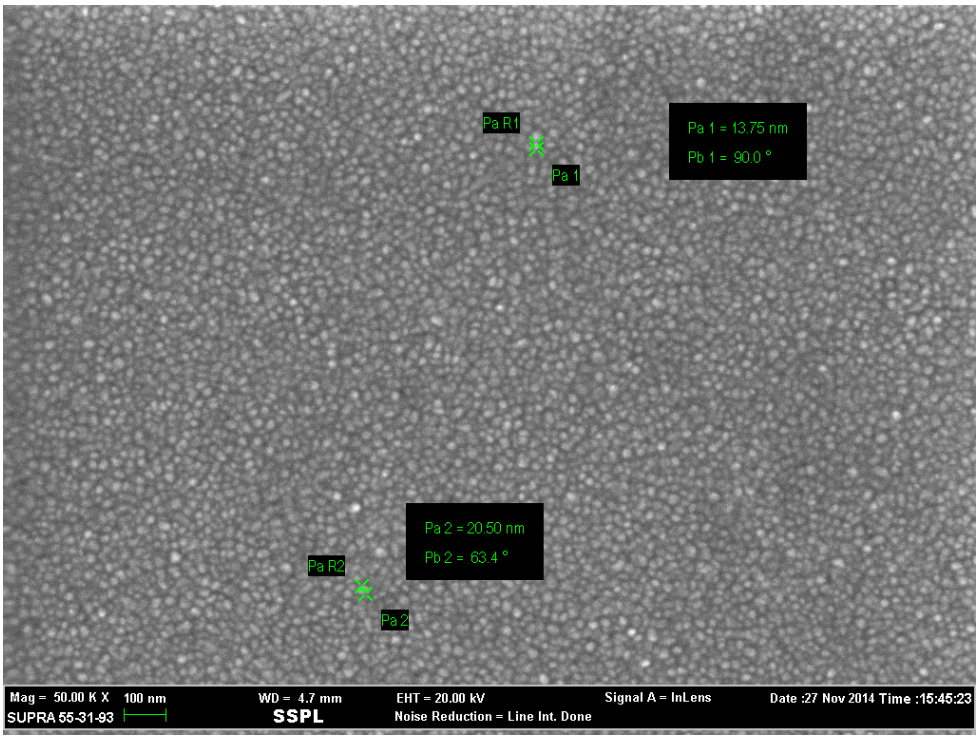

Figure 5.17 : SEM micrograph of gold at 50 KX magnification

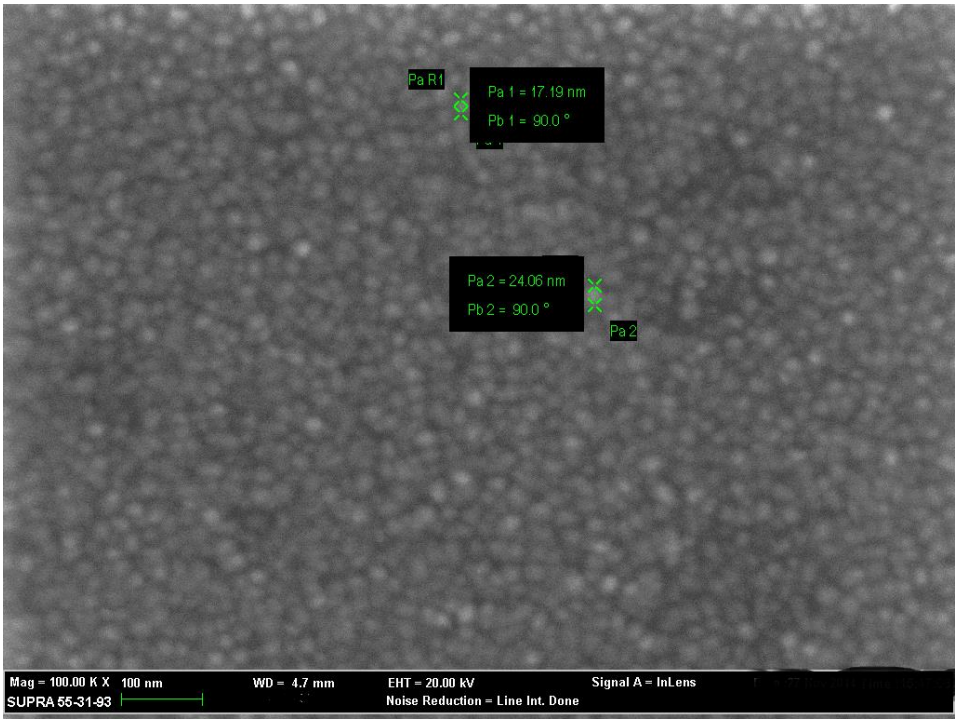

Figure 5.18 : SEM micrograph of gold at 100KX magnification

Figure 5.19 shows the XRD analysis of gold and shows the polycrystalline face centered cubic structure with preferential (111)plane.

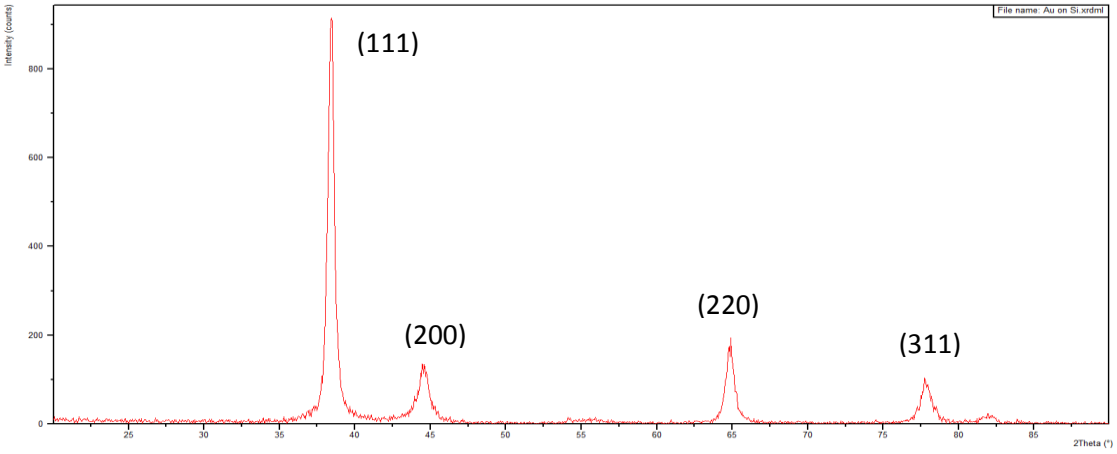

Figure 5.19 : XRD analysis of gold on silicon

The SEM micrographs shown in figure 5.20, 5.21 are at 5KX,10KX magnifications while fig.5.22, 5.23 are at 25KX magnification,20KV EHT, working distance 10.6mm to go through better study and analysis of grain size and structure. The SEM revealed the growth of 200nm-1μm grains size.

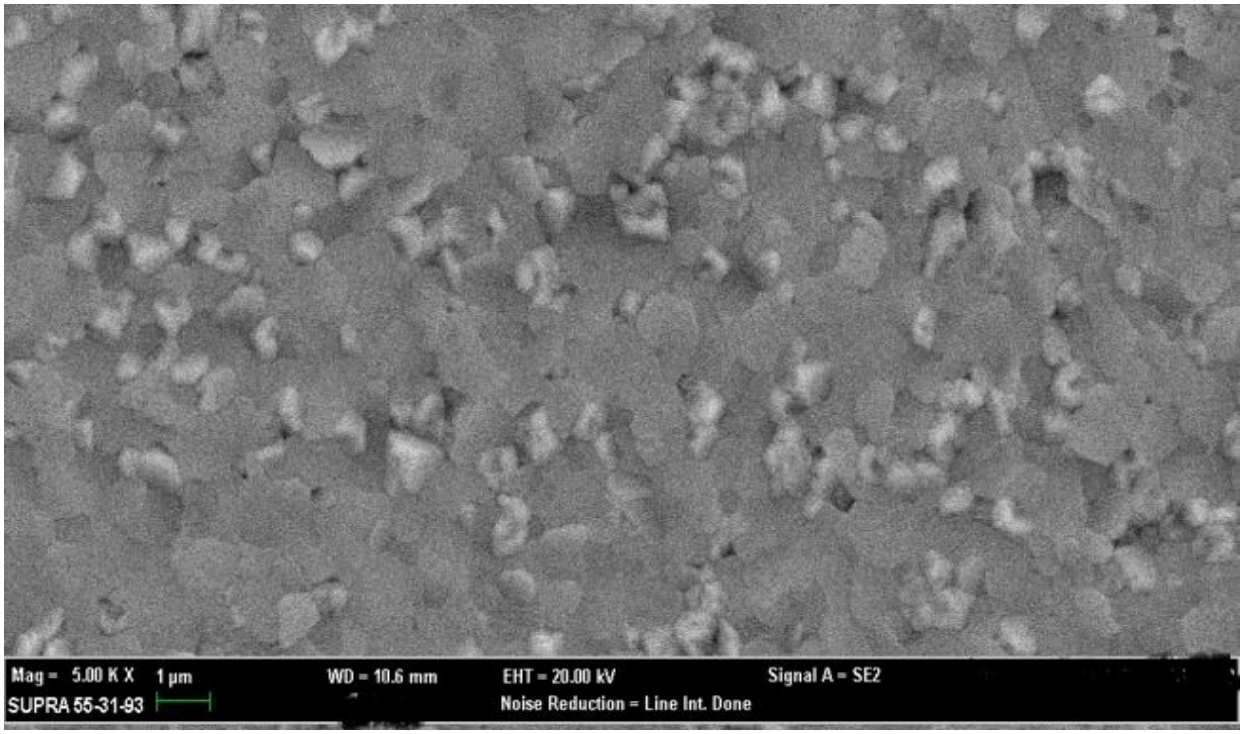

Figure 5.20: SEM Micrographs of Tin at 5X magnification

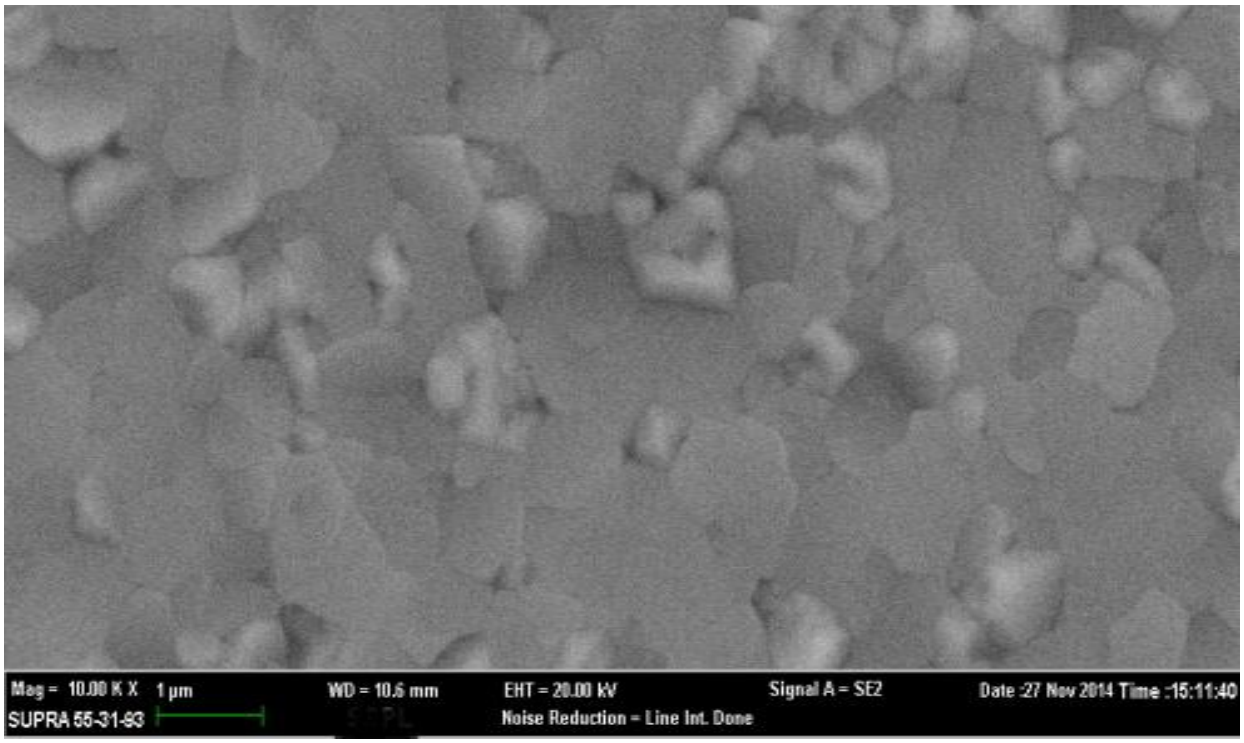

Figure 5.21: SEM Micrographs of Tin at 10X magnification

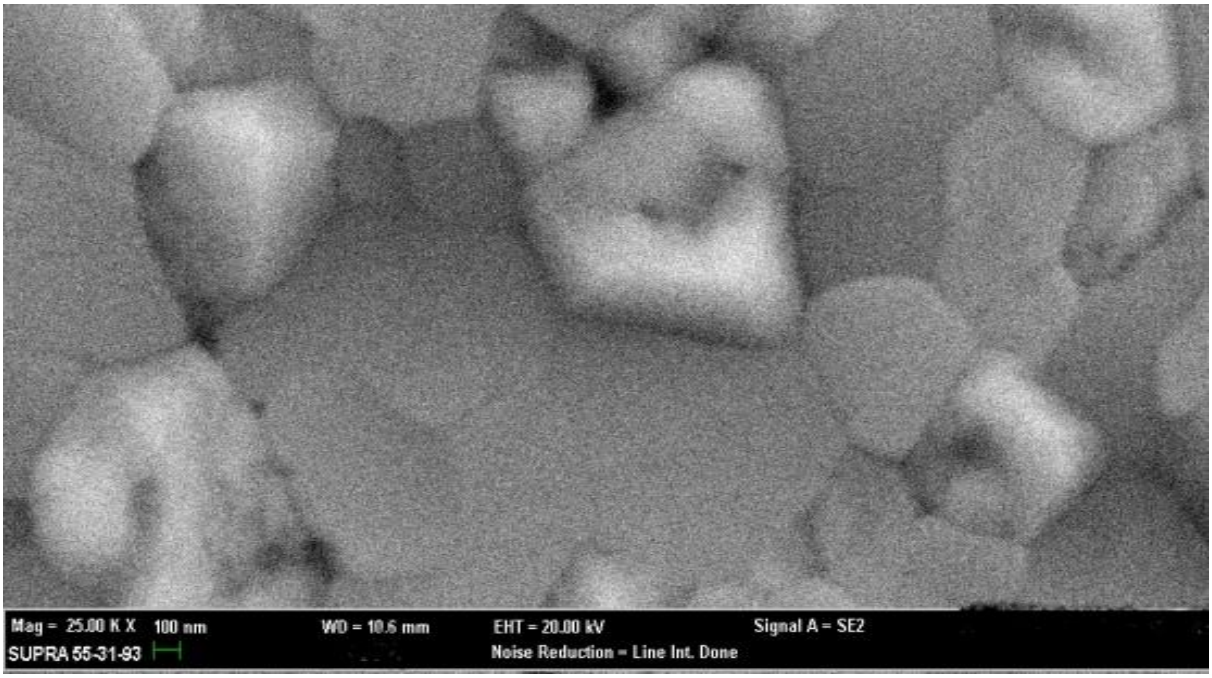

Figure 5.22 : SEM Micrographs of Tin at 25X magnification

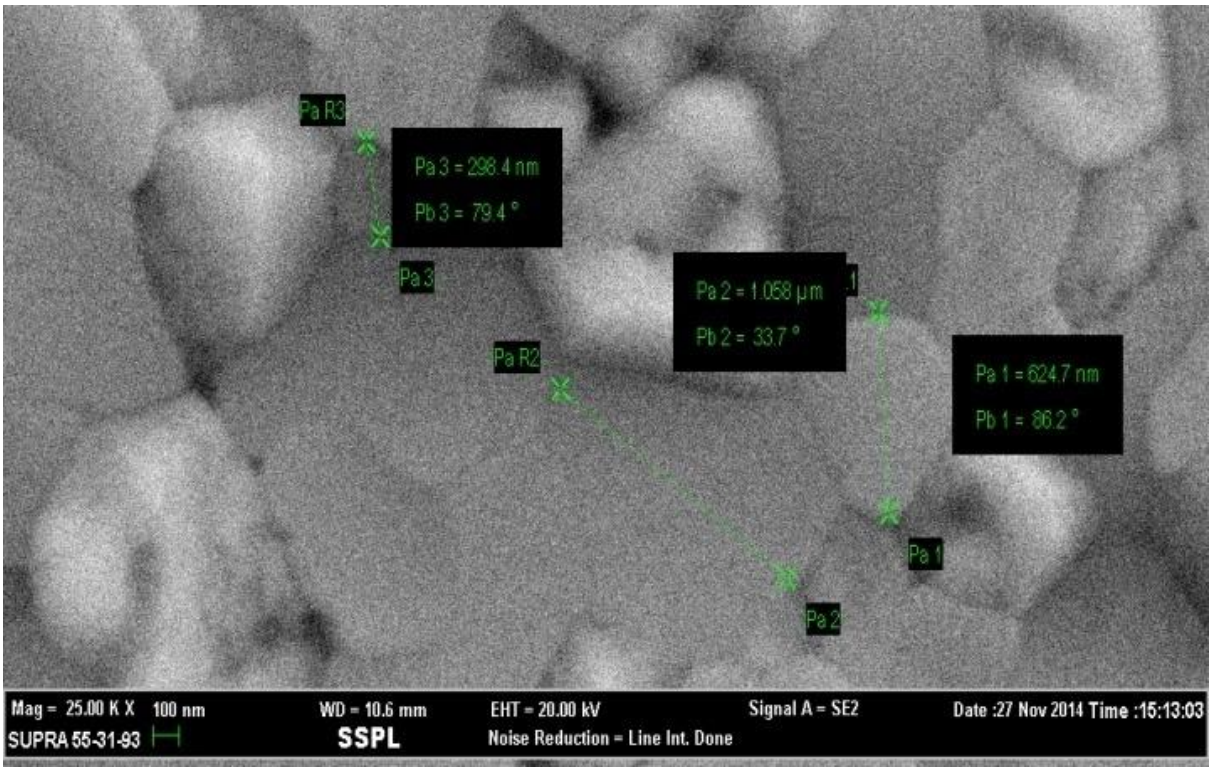

Figure 5.23 : SEM Micrographs of Tin at 25X magnification

Figure 5.24, 5.25 shows the SEM micrographs of Indium deposition on silicon substrate at 5KX,10KX magnification,20KV EHT,working distance 8.5mm for study the microstructure and grain size and shows the grain sizes 10-200nm with coarse dispersion on the surface.

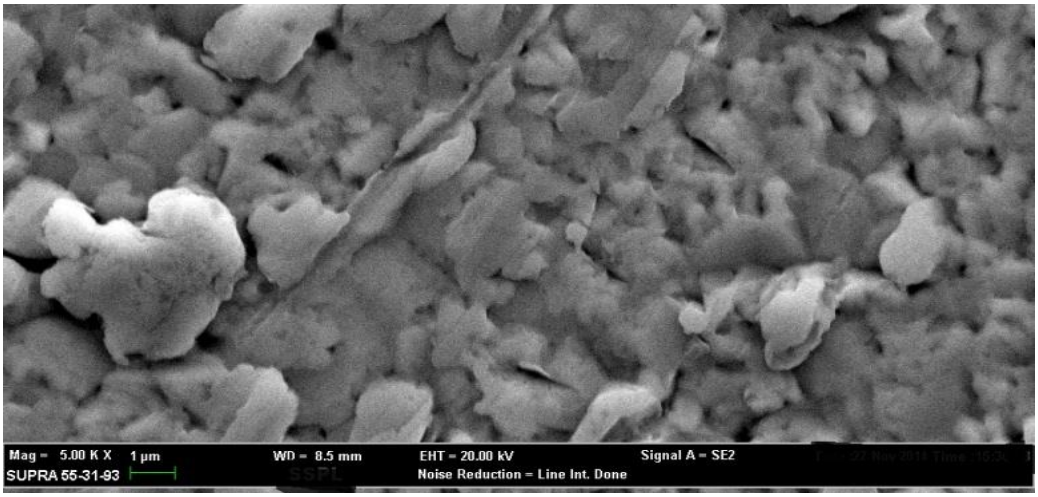

Figure 5.24 : SEM Micrographs of Indium at 5X magnificaio

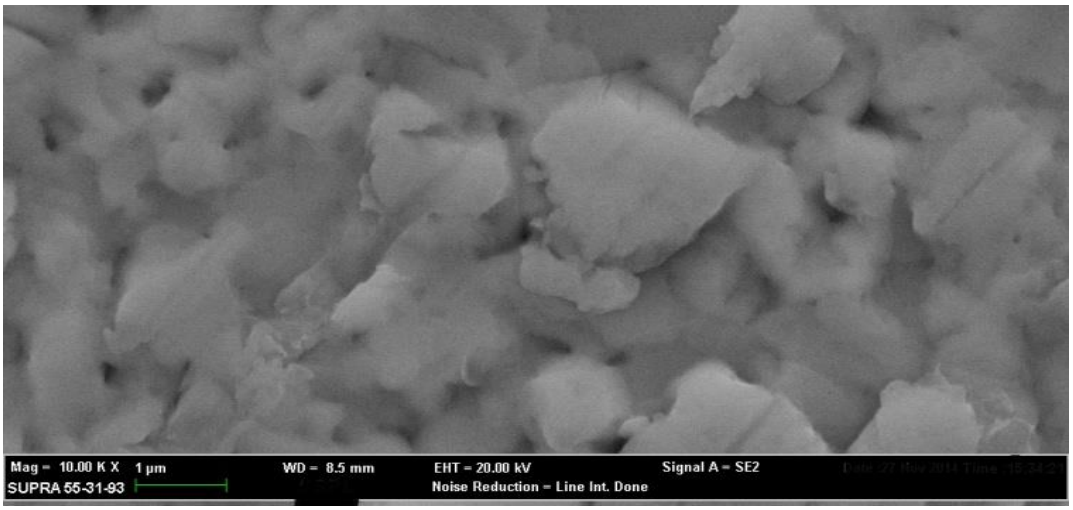

Figure 5.25: SEM Micrographs of Indium at 10X magnification

Figure 5.26 shows the XRD analysis by using Kα (wavelength 1.541874) of tin on silicon which shows that it is polycrystalline tetragonal structure preferential (101) plane with multiple peaks at 2θ angle

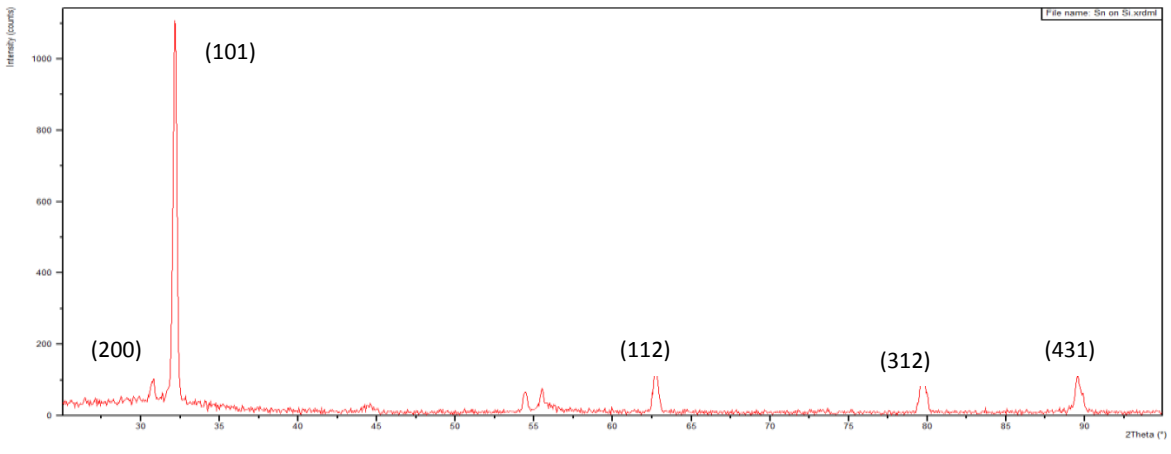

Figure 5.26: XRD analysis of Tin on silicon

Similarly, the XRD analysis of Indium on silicon for 183 nm thickness is shown in figure 5.27 which shows different peaks of intensity at different 2 angle revealing the polycrystalline tetragonal bcc structure with preferential (103) plane**.**

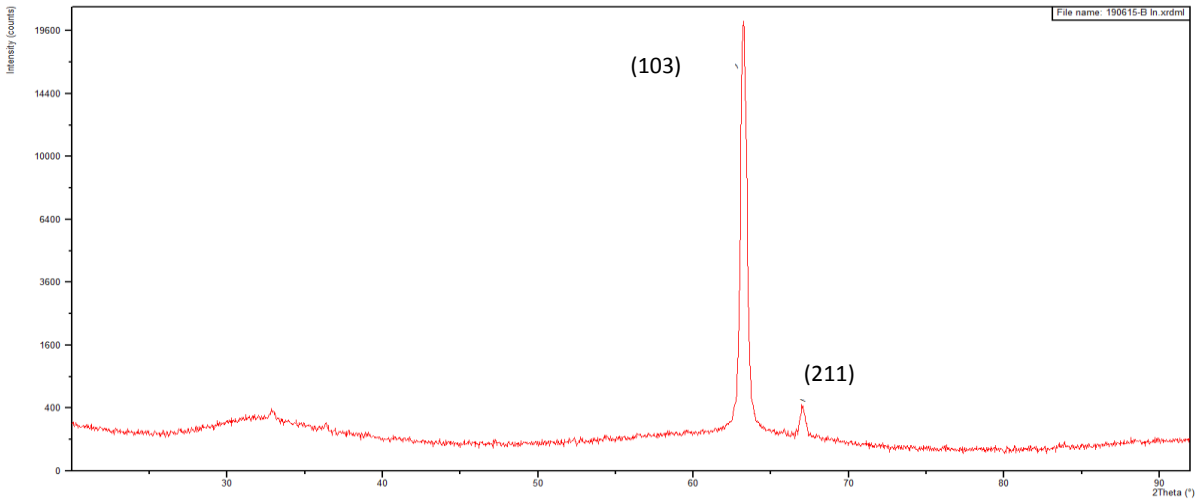

Figure 5.27 : XRD analysis of Indium on silicon

Measurement of deposited film thickness for gold, tin & indium 380,1650 &1830 Å respectively from Dektek surface profiler & comparison with thickness value given by Digital thickness monitor(DTM), a piezoelectric transducer.

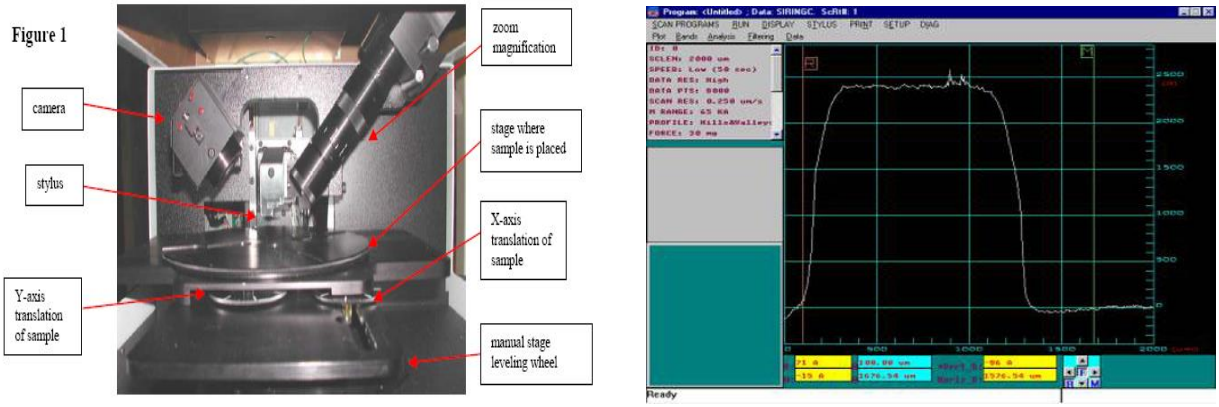

Figure 5.28 : dektek surface profiler

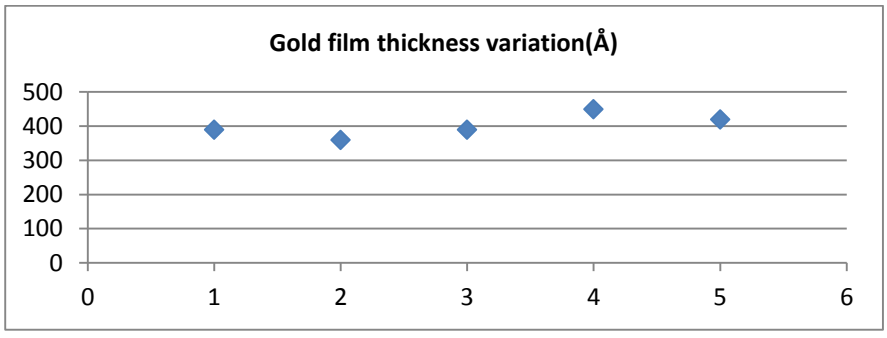

Figure 5.29: measurement of gold film thickness at 5 points by dektek

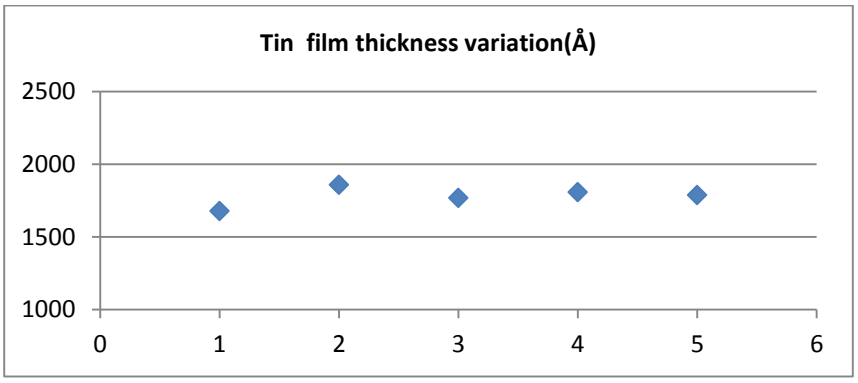

Figure 5.30 : measurement of tin film thickness at 5 points from dektek

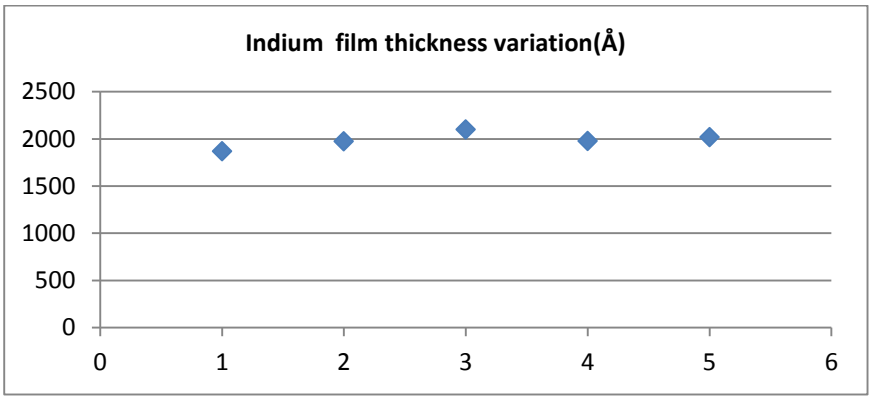

Figure 5. 30: measurement of indium film thickness at 5 points from dektek

From above measurement results it shows that in case of gold where thickness is less variation is not more than 5% while for tin and indium this variation is 10-15% .Thus overall variation in thickness in general is 5-15% from the value given by DTM(piezoelectric transducer) during process. This variation in thickness is obvious since the locations of quartz crystal and substrate are different inside the vacuum chamber & this variation can be minimized by keeping them close together.

Chapter 6

CONCLUSION & FUTURE WORK

6.1 Conclusion

For Optimized Methods for Fast and Accurate Simulations, gases at low pressures cannot be modeled using conventional computational fluid dynamics tools or DSMC method. That is due to the fact that kinetic effects become important as the mean free path of the gas molecules becomes comparable to the length scale of the flow. Thus angular coefficient method using time dependent BDF solver is very fast, accurate and easy to use in these conditions. Coatings of gold, tin & indium having good uniformity & appropriate thickness have been produced on stationary, non-rotated, flat substrates using a vacuum thermal evaporation technique that incorporates the use of a resistively heated molybdenum boat. The thickness uniformity around the substrate was a sensitive function of the mean free path as well as evaporant incidence angle. Also to increase the rate of evaporation we have to raise the temperature of the source. Thus this work presents the thermal evaporation of gold, tin and indium on silicon with thickness of 34-38nm, 144-165 nm and 160-183 nm respectively. The mass deposition of gold for 60 sec is 5.8×10^{-6} kg and mass transfer rate is 9.9×10^{-8} kg/sec. Gold is polycrystalline with fcc structure with preferential (111) plane. The average grain size is 12-30 nm with good, smooth and better dispersion on silicon. For tin mass deposited is 10.5×10^{-6} kg and mass transfer rate is 17.8×10^{-8} kg/sec. Tin is polycrystalline with tetragonal bcc structure in preferential (101) plane. Similarly, indium mass deposition for 60sec is 10.4×10^{-6} kg and mass transfer rate is 17.7×10^{-8} kg/sec. Tin has tetragonal bcc structure with (103) plane and grain size is 200 nm- 1μm. From above measurements it is concluded that variation in thickness in general is 5-15% from the value given by DTM(piezoelectric transducer). This variation in thickness is obvious since the positions of substrate and quartz crystal are at different locations in the vacuum chamber.

6.2 Future work

The future work will be to optimize the deposition conditions for heat and mass transfer during thermal evaporation of some other materials like CdTe, ZnS, CdS etc. and to improve the physical, optical & electrical properties to be used in solar cell, gas sensing applications, semi-conductor device fabrication etc. The study heat and mass transfer may be done for thin film deposition by sputtering and electron beam process. Study can further be done by varying deposition conditions like substrate heating, varying deposition rates etc on different substrates like glass, HgCdTe etc.

REFERENCES

[1] Ali Moarrefzadeh et.al. , Simulation and Modeling of Physical Vapor Deposition (PVD) Process,Wseas Transactions on Applied and Theoretical Mechanics, 7(2), 2012

[2] Adeleh Granmayeh Rada,Hamed Abbasib,Mohammad Hossein Afzalib, Gold Nanoparticles: Synthesising, Characterizing and Reviewing Novel Application in Recent Years Physics Procedia 22 , 2011 pp 203 – 208

[3[Ragini Raj Singh, et.al, Investigation of passivation processes for HgCdTe/CdS structure for infrared application, vol. 510, 2006, pp 235–240

[4] Wenjun Zhou et al. , Effective Permittivity of Ultrathin Chemical Vapor Deposited Gold Films on Optical Fibers at Infrared Wavelengths, J. Phys. Chem. C, 118, 2014, 670−678

[5] Keewah Chan et al. , Formation of gold nanoparticles in silicon suboxide films prepared by plasma enhanced chemical vapour deposition, journal of thin solid films , vol. 519 , 2011 , pp. 4952-4957

[6] Carl E. Larson et al. ,Chemical Vapor deposition of Gold , IBM Almaden Research Center, San Jose, California 95120 , August 11, 1986.

[7] Miroslav Gojo et al., Electrochemical Deposition of Gold in Citrate Solution Containing Thallium Polja~eka, Acta Chim. Slov. 2008, 55, 330–337 Received: 12-10-2007 Scientific paper

[8] Anne-Felicie Lamic-Humblot, et.al, An easy way to obtain thin film on silica glass substrate by chemical method, vol. 539, 2013, pp 151–153

[9] T. Donnelly, S. Krishinamurthy, K. Carney, N. McEvovy, J.G. Lunney , Pulsed laser deposition of Nanoparticles of film Au, Journal of Applied Surface Science, vol. 254, 2007 , pp 1303–1306

[10] X.Zhang, X. Zhang, S.S. Chu, J.R. Ho, C.P. Grigoropoulos, Excimer laser ablation of thin gold fims on a quartz crystal microbalance at various agron background pressures, Journal of applied physics A, vol. 64, 1997, pp 545-552

[11] Anna Schaub, Petr Slepicka, Irena Kasparkova, Petr Malinsky ,Gold Nanolayer and Nanocluster coatings induced by heat treatment and evaporation technique, Springer Open Journal, Nanoscale Research letters 2013, 8 : 249

[12] Behrang Moazzez, Stacey M. O'Brien and Erika F. Merschrod S., Improved Adhesion of Gold Thin Films Evaporated on Polymer Resin: Applications for Sensing Surfaces and MEMS, Journal of Sensors , vol. 13, 2013, pp 7021-7032

[13] Maxime Gougis1, Antonio Pereira2, Dongling Ma1 and Mohamed Mohamedi, Oxygen Gas

Assisted Laser Deposition of Gold Thin Films: Electrooxidation of Glucose, International Journal of Electrochemical Science, vol. 9, 2014, pp. 3588-3601

[14] C. Celed´on, M. Flores ,P. H¨aberle , and J. E. Vald´es, Surface Roughness of Thin Gold Films and its Effects on the Proton Energy Loss Straggling, Brazilian Journal of Physics, vol. 36, no. 3B, September, 2006, pp 956-959

[15] Hartmann Hieber, Karin Pape, Ageing of Thin Gold Films, Gold Bull., 1982, 15, (3)

[16] Adam Proszkynski, Dariusz Chocyk, Grzegorz Gladyszewski, Stress modification in gold metal thin films during thermal annealing, Optica Applicata, Vol. XXXIX, No. 4, 2009, 705-710

[17] C. R. Zamarreñoa et al. Optical Fiber Refractometers based on Indium Tin Oxide Coatings with Response in the Visible Spectral Region

[18] Souad Laghrib et al. , Tin oxide thin layers obtained by vacuum evaporation of tin and annealing under oxygen flow, Vacuum 82 (2008) 782-788

[19] Sea-Way Jan and Si-Chen Lee , Preparation and Characterization of Indium-Tin-Oxide Deposited by Direct Thermal Evaporation of Metal Indium and Tin ,Vol 134 , No 8 , J. Electrochemistry. Soc.: Solid State Science and Technology, August 1987

[20] D.Bruce Buchholz et.al, Differences between amorphous indium oxide thin films; Progress in Natural Science : Materials International 2013;23(5) :475-480

[21] Alexandru C.Fechete et al., Growth of Indium Oxide Nanostructures by Thermal Evaporation, Sensor Technology lab.,RMIT university,Australia, 1-4244-0453-3/06/$20.00@2006 IEEE

[22] C.A.Pan , T.P.Ma , High quality transparent conductive indium oxide films prepared by thermal evaporation, Appl. Phys. Lett. 37(2), 15 July 1980, American Institute of Physics

[23] B.Maniscalco, P.M. Kaminski, J.M. Walls, Thin film thickness measurement using Scanning White Light Interferometry 550(2014) 10-16

[24] M.Trzcinski et al , Alloy formation of ultrathin indium and silver layers onW(100) : A photoemission study, Material Science 589 (2005) 192 -200

[25] D. Kalhor, S.A. Ketabi, A. Ebrahimzad, M. Moosa Rezaei ,Annealing Effects on Opto-electronic Properties of Thermally-evaporated ITO/Ag/ITO Multilayered Films for Use in Color Filter Electrodes, World Applied Sciences Journal , vol. 6 (1), 2009 , pp 83-87

[26] Mika Yamaguchi , Ari Ide-Ektessabi , Hiroshi Nomura , Nobuto Yasui ab , cc , Characteristics of indium tin oxide thin films prepared using electron beam evaporation, Journal of Thin Solid Films vol. 447–448 , 2004 , pp. 115–118

[27] Artorn Pokaipisit, Mati Horprathum and Pichet Limsuwan, Influence of Annealing Temperature on the Properties of ITO Films Prepared by Electron Beam Evaporation and Ion-Assisted Deposition, Kasetsart Journal of Natural Science, vol. 42, 2008, pp 362 - 366

[28] P.S.Raghupathi, Joseph George and C.S.Menon, The Effect of Deposition Rate on Electrical, Optical and Structural Properties of ITO Thin Films, E-Journal of Chemistry, Vol. 2, No. 3, June

2005, pp 171-177

[29] Haichuan Mu, Hui Shen and David Klotzkin ,Dependence of film morphology on deposition rate in ITO/TPD/Alq_3/Al organic luminescence diode, Journal of Solid-State Electronics, vol. 48 , 2004 , pp. 2085–2088

[30] G.H. Gilmer et.al. , Thin film deposition: fundamentals and modeling, Journal of Computational Materials Science 12,1998, 354-380

[31] Authur K.Burak Ucer, Vacuum evaporation, www.users.wfu.edu

[32] F. Celestini and F. Mortessagne, " Cosine Law at the Atomic Scale : Toward Realistic Simulations of Kunden Diffusion, " Physics Rev. E, Vol. 77, 021202 , 2008

[33] J.M. Lafferty, Foundations of Vacuum Science and Technology, Wiley Interscience, 1998

[34] J.F. O'Hanlon, A User's Guide to Vacuum Technology, Wiley Interscience, 2003

[35] Book on 'Vacuum Deposition of Thin Films, L. Holland, F. Inst. P.,Publisher : Chapman and Hall ltd. , pp 144-145

[36] R.S. Mishra, Shailendra Kumar Gaur, Modeling &Simulation of Nano film thickness of Gold deposited by Thermal Evaporation Process (TEP), International Journal of Advance Research and Innovation, Volume 2 , 2014, pp 505-510

[37] Shailendra Kumar Gaur, R.S. Mishra, Thermal Evaporation- Modeling and Microstructure Studies of Indium and Tin Deposition, International Journal of Advance Research and Innovation, Volume 3, Issue 1, 2015, pp 207-215

[38] Shailendra Kumar Gaur, R.S. Mishra, Modeling of Inductively Heated Copper Cylinder with Water Cooling Based on Turbulent Flow and Instantaneous Mixing, International Journal of Advance Research and Innovation, Volume 2, Issue 3 ,2014, pp 582-585

[39] CIIMS Applied Physics-lectures

Appendix A

Table A.1 Typical Boat /Crucible Material

Refractory Metals		
Material	**Melting Point (°C)**	**Temperature for 10-mtorr Vapor Pressure (P_e) (°C)**
Tungsten (W)	3380	3230
Tantalum (Ta)	3000	3060
Molybdenum (Mo)	2620	2530
Refractory Ceramics		
Graphitic Carbon (C)	3799	2600
Alumina (Al_2O_3)	2030	1900
Boron Nitride (BN)	2500	1600

Appendix B

LIST OF PUBLICATIONS

1. 'Modeling &Simulation of Nano film thickness of Gold deposited by Thermal Evaporation Process (TEP)' , R.S. Mishra, Shailendra Kumar Gaur, International Journal of Advance Research & Innovation, Volume 2, 2014, pp 505-510

2. 'Modeling of Inductively Heated Copper Cylinder with Water Cooling Based on Turbulent Flow and Instantaneous Mixing', Shailendra Kumar Gaur, R.S. Mishra, International Journal of Advance Research & Innovation, Volume 2, Issue 3, 2014 , pp 582-585

3. 'Thermal Evaporation- Modeling and Microstructure Studies of Indium and Tin Deposition' , Shailendra Kumr Gaur, R.S. Mishra, International Journal of Advance Research & Innovation, Volume 3, Issue 1 , 2015, pp 207-215